



FINAL PROJECT REPORT

PROJECT TITLE:
DEVELOPMENT OF A SELF-SUSTAINED WIRELESS INTEGRATED STRUCTURAL
HEALTH MONITORING SYSTEM FOR HIGHWAY BRIDGES

COOPERATIVE AGREEMENT # RITARS11HUMD

University of Maryland with North Carolina State University and URS



ACKNOWLEDGEMENTS

This project final report was developed as part of the project funded and supported from the U.S. Department of Transportation, Office of the Assistant Secretary for Research and Technology (USDOT/OST-R)- Cooperative Agreement RITARS11HUMD. The methods, results, opinions, and statements contained in this report are findings of the research team and do not represent the official policy or position of the U.S. Department of Transportation, Office of the Assistant Secretary for Research and Technology.

The authors wish to thank the Maryland Department of Transportation (MDOT) and the North Carolina Department of Transportation (NCDOT) for partnering and contributing to the research project. Special thanks are also due to the members of the FHWA-led Advisory Panel who all provided time, expertise, guidance, and direction to the accomplishment of project technical scope and objectives.

EXECUTIVE SUMMARY

Fatigue-induced cracking is a common failure mode in many steel bridges reaching their original design life. These aging bridge structures have experienced increasing traffic volume and weight, deteriorating components as well as a large number of stress cycles. In Maryland alone, there are a number of cases reported that involve fatigue damage in highway bridges. Nationally, in 2009, fatigue cracking induced damages to the eye-bars of the recently replaced San Francisco Bay Bridge led to pieces of steel plummeting onto the roadway during rush hour. Several steel repair parts fell on peak hour traffic as wind caused the bridge to vibrate and the traffic was stopped. Such incidences happen frequently without prior warnings.

The investment of the United States in civil infrastructures is estimated to be \$20 trillion. The magnitude of the societal challenges associated with infrastructures, especially with aging bridges, is daunting. The Commercial Remote Sensing and Spatial Information (CRS&SI) Technologies Program authorized in the Safe, Accountable, Flexible and Efficient Transportation Equity Act: A Legacy for Users (SAFETEA-LU) focuses on major national initiatives and validation of CRS&SI technology applications which deliver smarter and more efficient methods, processes and services for transportation infrastructure development and construction. Despite years of research in overcoming these challenges, catastrophic failures (e.g., the interstate 35W bridge collapse in Minneapolis, MN in 2007) still occur, which is mainly due to various difficulties in detecting bridge health conditions under highly uncertain operational conditions and also our limited understanding of the failure mechanisms in these systems. This project strives to address this issue by establishing an Integrated Structural Health Monitoring (ISHM) System for remote infrastructure sensing, diagnostics and prognosis. The ISHM entailed a few recent

innovations that transformed the current state-of-the-practice in remote sensing and management of highway infrastructures.

The novelty and uniqueness of the technologies of this project are summarized into the following five thrust areas:

Thrust 1: Reconfigurable sensor dots (sensor technology)

Thrust 2: Passive interrogation of evolving damage (AE diagnostics)

Thrust 3: Hybrid-mode energy scavenger (energy harvesting) to power wireless sensor

Thrust 4: Multi-media wireless smart sensor (Wireless sensing)

Thrust 5: Prognostics

There are six tasks involved in this project, which are:

Task 1: Establishing weak point identification maps and conducting baseline field tests

Task 2: Fabrication and characterization of piezo paint AE sensor with reconfigurable sensing dots

Task 3: Development of a time-reversal (T-R) method for AE source identification

Task 4: Development of a wireless smart sensor with a hybrid-mode energy harvester and embedded T-R algorithms

Task 5: Developing ISHM in both laboratory and field environments and implementation with Bridge Management System

Task 6: Project Website, Report and Project Assessment

In summary, a functioning wireless Integrated Structural Health Monitoring (ISHM) System with remote sensing, diagnostics and prognosis was developed, tested in the lab as well as in the field, deployed and validated. A project website (<http://ishm.umd.edu/>) hosted at the UMD

was established at the onset of the project and kept updated throughout. Quarterly reports were submitted starting from July 15th, 2011. This final progress report summarizes the results of the technical assessment and evaluation and is submitted as deliverable of this project. Also this report discusses the results of the economic evaluation of the project. The MDDOT and NCDOT provided in-kind supports to implement the technology and make the system ready for commercialization. Strategy of commercialization has been consulted to the Offices of Technology Commercialization (OTC) of UMD and NCSU, and other DOTs.

Guests from the Maryland Department of Transportation were invited to the demo site at I-95 over Patuxent River, Laurel, MD. The whole process was performed to showcase the wireless smart sensor system with piezo paint AE sensors and hybrid-mode energy harvester. Also demonstrated were the pencil break tests to simulate the fatigue cracks to different groups of guests from Maryland State Highway Administration (MDSHA) and Maryland Transportation Authority (MDTA). The open day on May 22nd, 2014 was to demonstrate the AE sensor and crack detection technology and explain the benefits of the system to the bridge owners.

Table listed below is the summarization of the final status of twelve deliverables based on the extended 36-month period.

Summary of the Final Status of Twelve Deliverables	
Deliverable	Item
1	<ul style="list-style-type: none"> • The technical advisory committee (TAC) was formed and kick-off team meeting was conducted on August 5, 2011. • Baseline field test procedure on Paint Branch Bridge on US Route 1 was conducted in the first quarter to experimentally determine the environmental and bridge parameter values for ISHM system. • Remote sensing requirements and prognostics procedure for the proposed ISHM system were developed in the first quarter.
2	<ul style="list-style-type: none"> • Project website hosted at the University (ishm.umd.edu) was established in the first quarter and periodically updated throughout the project period

(2011-2014)	
3	<ul style="list-style-type: none"> Findings of the all activities performed under Task 1 (finite element model, sensor placement scheme, environmental variable data, etc.) and details of baseline test on the Paint Branch Bridge on US Route 1 were reported and made available on the project website in the second quarter.
4	<ul style="list-style-type: none"> Findings of the all activities performed under Task 2 (piezo paint sensor with improved sensitivity, reconfigurable piezo paint sensor dots), description of corresponding development procedure for modeling, fabrication, and experimental characterization of piezo paint AE sensor were reported and made available on the project website from the second to the fourth quarters.
5	<ul style="list-style-type: none"> The status of research efforts and findings in virtual T-R experiments and lab tests to validate and characterize T-R method for fatigue related damage detection were reported periodically throughout the project.
6	<ul style="list-style-type: none"> Self-sustained wireless smart sensor and hybrid-mode energy harvester were developed in the extended third year. Findings of the all activities performed under this task were reported and made available on the project website from the eighth to the twelfth quarters
7	<ul style="list-style-type: none"> The status of research efforts and findings in wireless smart sensor and onboard diagnostics method based on the T-R algorithm were reported. The wireless smart sensor system were validated and evaluated through corresponding lab tests. Both works described above were extended to the third year, reported and made available on the project website from the eighth to the twelfth quarters.
8	<ul style="list-style-type: none"> Integrated piezo paint AE sensors with wireless smart sensor and hybrid-mode energy harvester were validated and thoroughly evaluated through lab tests and field tests on real bridges The work was extended to the third year, reported and made available on the project website from the ninth to the twelfth quarters.
9	<ul style="list-style-type: none"> The research efforts and findings in lab tests and field tests of the ISHM system were extended to the third year, reported and made available on the project website from the ninth to the twelfth quarters.
10	<ul style="list-style-type: none"> Strategy to incorporate remote sensing and prognosis of bridge components into bridge management system was reported and made available on the project website in the sixth quarter. It has been thought through the whole project.
11	<ul style="list-style-type: none"> Quarterly status and progress reports were submitted every quarters of 2011- 2014 and final project report is enclosed.
12	<ul style="list-style-type: none"> 11 paper submissions to conference presentations and publications to TRB meeting or other conferences with recognition of this project (details in Chapter 6).

Table of Contents

Acknowledgement	2
Executive Summary.....	3
1.0 Introduction	8
2.0 Task 1: Establishing weak point identification maps and conducting baseline field tests..	18
3.0 Task 2: Fabrication and characterization of piezo paint AE sensor with reconfigurable sensing dots	22
4.0 Tasks 3 & 4: Development of a wireless smart sensor with a hybrid-mode energy harvester and embedded time-reversal (T-R) algorithms	31
5.0 Task 5: Developing ISHM in both laboratory and field environments and implementation with Bridge Management System	39
6.0 Task 6: Project Website, Report and Project Assessment	73
7.0 Findings/Conclusions	77

Attachment

1. The matrix listing tasks and deliverables with their milestone schedule r

1.0 Introduction

1.1 Background

Fatigue-induced cracking is a common failure mode in many steel bridges reaching their original design life. These aging bridge structures have experienced increasing traffic volume and weight, deteriorating components as well as a large number of stress cycles. In Maryland alone, there are a number of cases reported that involve fatigue damage in highway bridges. For example, cracks resulting from the typical web gap distortion near the bottom flange of welded plate girders were reported in the US 13 Bridge (a steel I-girder bridge) over Pocomoke River, Maryland (Zhou, 2006). The distortion induced stresses have initiated horizontal cracks in the web-to-flange welds and propagated into vertical cracks at the end of the web-to-connection plate welds. On March 14 2003, two large cracks were discovered in the webs of two steel girders on the I-895 Bridge over U.S. Route 1 and the Patapsco River in Elkridge, Maryland (Zhou and Biegalski, 2010). The fracture originated at the top of the web-to-stiffener weld. One crack propagated downward and diagonally, fractured the full height of the 90-inch web plate. Nationally, in 2009, fatigue cracking induced damages to the eye-bars of the recently replaced San Francisco Bay Bridge led to pieces of steel plummeting onto the roadway during rush hour. Several steel repair parts fell on peak hour traffic as wind caused the bridge to vibrate and the traffic was stopped. Such incidences happen frequently without prior warnings. The recent Steel Bridge Testing Program (SBTP) supported by FHWA is aimed at evaluating and improving “off-the-shelf” NDT technologies capable of detecting surface and subsurface fatigue cracks in steel bridges (Haldipur and Jalinoos, 2010 a and b).

The investment of the United States in civil infrastructures is estimated to be \$20 trillion. The magnitude of the societal challenges associated with infrastructures, especially with aging bridges, is daunting. The Commercial Remote Sensing and Spatial Information (CRS&SI) Technologies Program authorized in the Safe, Accountable, Flexible and Efficient Transportation Equity Act: A Legacy for Users (SAFETEA-LU) focuses on major national initiatives and validation of CRS&SI technology applications which deliver smarter and more efficient methods, processes and services for transportation infrastructure development and construction. Despite years of research in overcoming these challenges, catastrophic failures (e.g., the interstate 35W bridge collapse in Minneapolis, MN in 2007) still occur, which is mainly due to various difficulties in detecting bridge health conditions under highly uncertain operational conditions and also our limited understanding of the failure mechanisms in these systems. This project strives to address this issue by establishing an Integrated Structural Health Monitoring (ISHM) System for remote infrastructure sensing, diagnostics and prognosis. The ISHM entailed a few recent innovations that transformed the current state-of-the-practice in remote sensing and management of highway infrastructures: 1) interrogation of local small damages from wideband acoustic emission (AE) signals even in areas where traditional AE sensors cannot be placed due to geometry and structural constraints; 2) smart wireless sensor networks that can self-power (wind or solar), self-calibrate, and automatically scan and diagnose interrogation data.

1.2 Novelty of Project Research Results

The novelty and uniqueness of the technologies of this project are summarized into the following five thrust areas:

Thrust 1: Reconfigurable Sensor Dots (Sensor Technology): A flexible, reconfigurable, high-

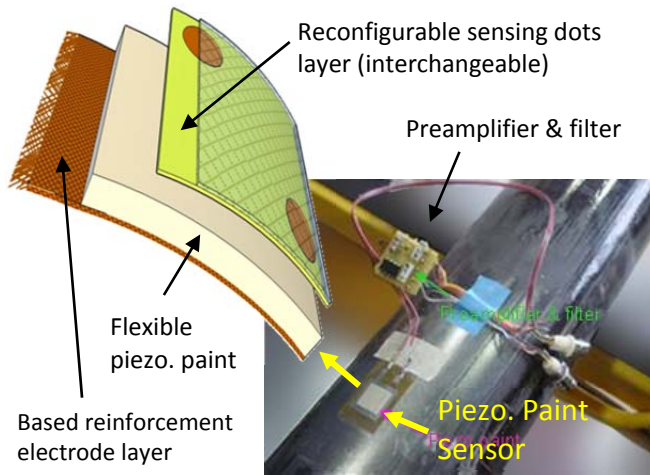


Figure 1 - Flexible piezoelectric paint sensor tested in the UMD Laboratory

fidelity piezo paint sensor (Figure 1) developed by the participating researchers at UMD is capable of sensing wideband AE signals in complex bridge structural components. Wide-band signal is essential to inverse waveform analysis to quantify the AE source (e.g., fatigue crack) characteristics. In particular, the piezo paint

sensor with reconfigurable sensor dot pattern offers a novel approach with a myriad of advantages: 1) low-profile, flexible film-like sensor that conforms to structures with complex geometry; 2) sensing dot pattern reconfigurable for different sensing algorithm requirements; and 3) wideband sensor with less signal distortion at the desired frequency band (40 kHz to 600 kHz).

Thrust 2: Passive Interrogation of Evolving Damage (AE Diagnostics): The participating

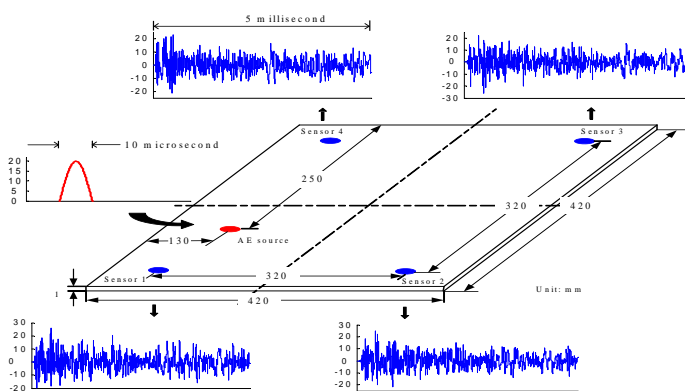


Figure 2 - Four multiply reflected sensor data under AE source

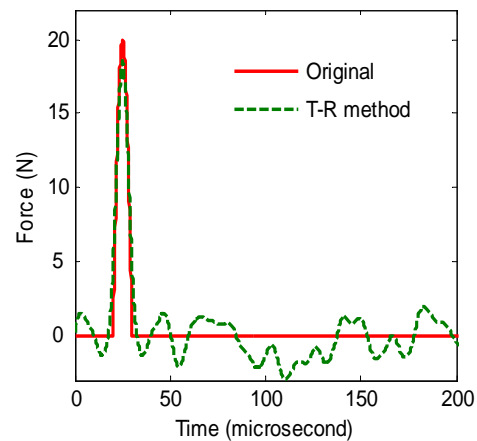


Figure 3 - AE loading history retrieved by T-R method.

researchers at NCSU have performed a feasibility study to unravel the AE location and AE loading time history using the T-R technique. An AE source is simulated by using an electric hammer hitting at one point inside a *finite* plate with duration 10 μ s. In the lab test a network of four sensors that are located near the corner of plate received the signal for the duration 50 ms shown in Figure 2. The sensor signals show complex waveforms due to over hundreds of boundary reflections. It can be seen that by using the T-R method all the received signals have traveled back and refocused at the source location (not shown here) and the loading history shown in Figure 3 is almost fully recovered. These lab test results showed that the T-R method may be used for illuminating the AE location and for recovering the original loading history in complex civil structures.

Thrust 3: Hybrid-mode Energy Scavenger (Energy Harvesting) to Power Wireless Sensor:

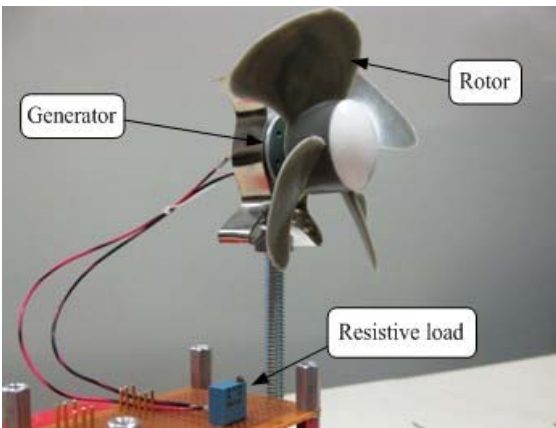


Figure 4 - Miniature Wind Turbine system developed by NCSU to harvest wind energy.

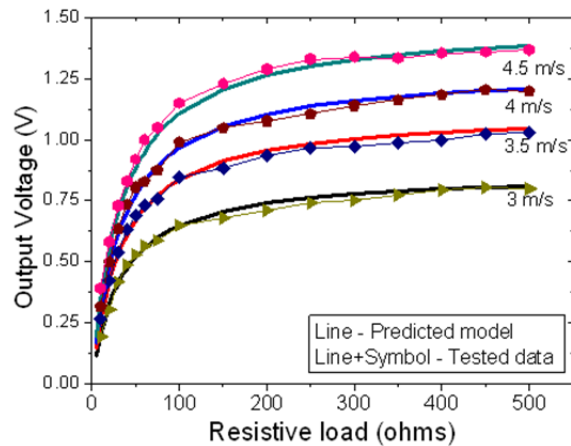


Figure 5 - Tested and predicted output voltage versus resistive load

The participating researchers at NCSU have conducted researches for energy harvesting using wind energy, specifically for applications in highways and bridges. A miniature wind turbine system (MWTS) composed of commercially available components was used for prototyping and

verification to harvest energy from ambient airflow (Figure 4). A 7.6 cm thorgren plastic propeller blade was adopted as the wind turbine blade. A maximum net efficiency of 14.8% and a maximum output power of 13.4 mW at a wind speed of 4 m/s (9 mph) were observed. A power density of up to 19 mW/cm³ at a wind speed of 8 m/s (18 mph) has been estimated (Figure 5).

A hybrid-mode energy harvester utilizing wind power from MWT and solar energy (specialized electronic board for voltage converting to be developed) were designed to power the wireless sensors for on-board signal processing and wireless communication among wireless sensors.

Thrust 4: Multi-media Wireless Smart Sensor (Wireless Sensing): The participating researchers

at NCSU developed the first wireless intelligent sensor platform (WISP) that is capable of

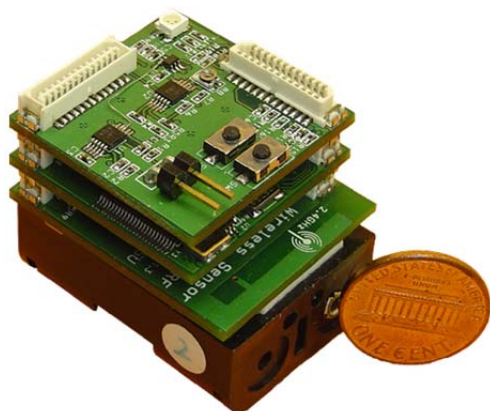


Figure 6 - A compact modularized high speed wireless sensor platform developed by NCSU researchers.

sensing acoustic emission (AE) signals (e.g. sampling rate up to 10MHz) while maintaining low power consumption. The sensor platform (Figure 6) has a dual-controller architecture and utilizes a FPGA (Field Programmable Gate Array) as a secondary controller to enable direct memory access. Average power consumption per sample is 20 times less than conventional sensors making N-sized batteries

sufficient for power sources. It has been verified that both power consumption and time duration for processing can be significantly lowered by improving I/O throughput. The research and knowledge previously developed have been transformed to the smart sensor for civil structures SHM applications in this project.

Note that the WISP adopted a hybrid architecture and utilized parallel logic processing to achieve sampling rate *hundred* times faster than conventional wireless sensor designs whereas power consumption is only increased about 4~5 times.

The transition of wireless monitoring system from the laboratory to the field test has been demonstrated by a member of research teams. A number of algorithms, including Fourier transform, wavelet transform, and system identification models, have been embedded in the wireless sensor.

Thrust 5: Prognostics: This Paris law with two damage parameters is used in steel bridges with fatigue type of failure. By incorporating the probabilistic structural deterioration model with Bayesian nets, more accurately updated structural reliability and remaining useful life (RUL) will be evaluated and optimal maintenance strategies will then be made accordingly. Using Bayesian updating from five diagnostic damage images, the damage parameter m in the Paris damage evolution law, $da/dN = C(\Delta K)^m$, rapidly converged with very narrow distributions (Figure 7).

With the updated m , the RUL in terms of number of fatigue cycles can be accurately predicted by

$$N = \int_{a_0}^{a_N} \frac{da}{C(\sigma\sqrt{\pi a})^m} = \frac{a_N^{1-m/2} - a_0^{1-m/2}}{C\sigma\sqrt{\pi}(1-m/2)}$$

1.3 Technical Approach and Project Deliverables

There are six tasks involved in this project, which are:

Task 1: Establishing weak point identification maps and conducting baseline field tests

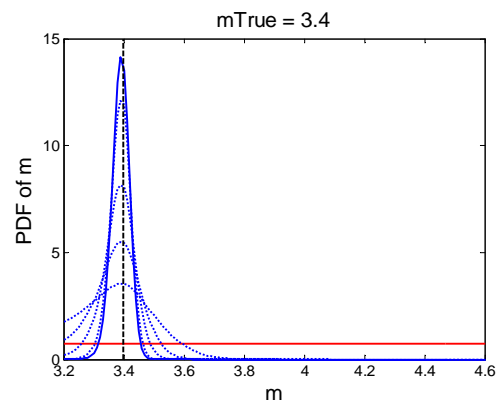


Figure 7 - Updated distribution of material parameter m for $m_{true} = 3.4$

Task 2: Fabrication and characterization of piezo paint AE sensor with reconfigurable sensing dots

Task 3: Development of a time-reversal (T-R) method for AE source identification

Task 4: Development of a wireless smart sensor with a hybrid-mode energy harvester and embedded T-R algorithms

Task 5: Developing ISHM in both laboratory and field environments and implementation with Bridge Management System

Task 6: Project Website, Report and Project Assessment

Twelve (12) project deliverables were identified in the Cooperative Agreement Attachment 2 and listed as follows:

1. Forming the technical advisory committee (TAC) and conducting kick-off team meeting (UMD, NCSU, URS, and MddOT). Determine baseline field test procedure to experimentally determine the environmental and bridge parameter values (noise level, energy intensity, measurement range, wind, moisture, traffic) to support sensor, wireless communication, energy harvester and ISHM system (software & hardware) design. Remote sensing requirements and prognostics procedure for the proposed ISHM system to be developed and integrated to Bridge Management Systems will also be determined in this kick-off team meeting. Results due to DOT within three (3) months of the effective date of the Agreement.
2. Establishing and updating project website hosted at the University. Initiation of the project website due to DOT within three (3) months of the effective date of the Agreement.

-
3. A report that includes the findings of the all activities performed under Task 1 (finite element model, sensor placement scheme, environmental variable data, etc.) and details of baseline test on the specified bridge. This will be prepared in accordance with the requirements of US DOT and made available on the project website. Reporting will be due to DOT within six (6) months of the effective date of the Agreement.
 4. A report that describes the findings of the all activities performed under Task 2 (piezo paint sensor with improved sensitivity, reconfigurable piezo paint sensor dots), description of corresponding development procedure for modeling, fabrication, and experimental characterization of piezo paint AE sensor. This report will be prepared in accordance with the requirements of US DOT and made available on the project website. Reporting will be due to DOT within twelve (12) months of the effective date of the Agreement.
 5. A report that documents the research efforts and findings in virtual T-R experiments and lab tests to validate and characterize T-R method for fatigue related damage detection. This report will be prepared in accordance with the requirements of US DOT and made available on the project website. Reporting will be due to US DOT within twelve (12) months of the effective date of the Agreement.
 6. An interim report on wireless smart sensor comprised of self-sustained wireless smart sensor and hybrid-mode energy harvester. Results will be due to DOT within twelve (12) months of the effective date of the Agreement as an interim report
 7. A report that documents the research efforts and findings in wireless smart sensor and onboard diagnostics method based on the T-R algorithm, as well as corresponding lab tests to validate and evaluate the wireless smart sensor system. This report will be prepared in

accordance with the requirements of US DOT and made available on the project website. Reporting will be due to US DOT within twenty-four (24) months of the effective date of the Agreement.

8. An interim report on piezo paint AE sensors integrated with wireless smart sensor and hybrid-mode energy harvester that are validated and thoroughly evaluated through lab tests and field tests on real bridges. Results will be due to DOT within thirty (30) months of the effective date of the Agreement.
9. A report that documents the research efforts and findings in lab tests and field tests of the ISHM system. This report will be prepared in accordance with the requirements of US DOT and made available on the project website. Reporting will be due to US DOT within thirty-six (36) months of the effective date of the Agreement.
10. A report that strategy to incorporate remote sensing and prognosis of bridge components into bridge management system will be recommended. Strategy of commercialization will also be established at this stage. A final report will be due to DOT within thirty-six (36) months of the effective date of the Agreement. Prior to the submission of the final report, a draft will be sent for review and comment.
11. Preparing and submitting quarterly status and progress reports and final project report in accordance with Article VI.F.2, 3, and 4 of the Basic Agreement.
12. Submitting paper to conference presentations and publication to TRB meeting or other pipeline conferences. Due to DOT within thirty-six (36) months of the effective date of the Agreement.

The matrix listing tasks and deliverables with their milestone schedule is defined in the attachment of this report. The project has been extended and approved from 24 months to 36 months. The final deliverable status and dates are shown in Chapter 6 of this report.

2.0 Task 1: Establishing weak point identification maps and conducting baseline field tests

The main goal of baseline field test is to plan the sensor locations and collect field data using currently available devices to support the design and future implementation of the piezo paint sensor dots, wireless communication, diagnostics, and energy scavenger technologies. Tests, led by UMD team, have been conducted on several steel bridges.

2.1 Task 1.1: Analyzing bridges

Baseline field tests were conducted on a steel bridge designated by the Maryland Department of Transportation (MDDOT). The I-68 over MD 55 Bridge No. 0111503, a medium length bridge, was identified in the proposal. Instead, Paint Branch Bridge on US Route 1 and I-270 over Middlebrook Road Bridge were selected since retrofit works were planned and they are good candidates to detect the fatigue growth before and after the repair of this fracture-critical bridge that carries frequent heavy-move vehicles - up to 380,000 lbs in gross weight (Zhou, 2010). In the proposal the Bay Bridge was the candidate for long-span bridges where some fatigue retrofits were designed recently and the construction is on-going (Figure 8).

Then, due to the state's inspection and construction schedule, alternate bridge, I-95 over Patuxent River Bridge was selected. Bridge was first analyzed through finite element analysis. The results were compared with field test

data for verification. This task also obtained global and local

failure maps for weak point identification using the computer (or simulation) models of bridge systems. Inspection data of the bridge was utilized in order to incorporate the true global and

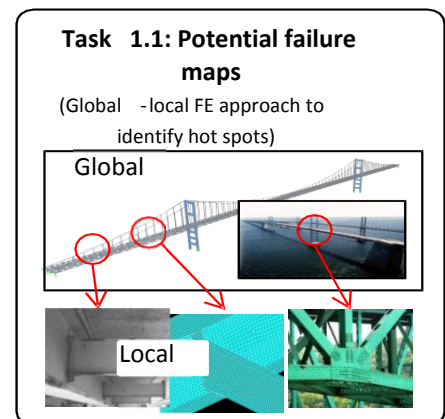
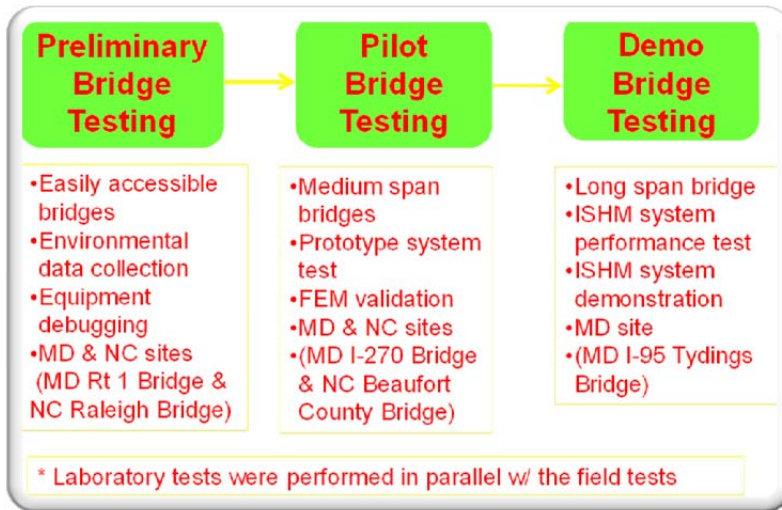


Figure 8 - Potential Failure Map through FEM Analysis

local geometries and conditions into the computer models. Both global and local computational models were established for qualitative (pass or fail) and quantitative (degree of deterioration) evaluations of bridge system performances.



In selecting candidates for field experiments, three different categories with different purposes are set, which are named as (1) preliminary bridge testing, (2) pilot bridge testing, and (3) demo bridge testing. The three categories and their selecting criteria are listed in Figure 9.

Figure 9 - Field Experiment Bridge Candidates

2.2 Task 1.2: Sensor placement on the bridge

Sensor placement schemes for baseline field tests were determined based on finite element simulation results and consultation with experts with the goal of collecting desired environmental variable data. The power consumption of wireless communication and cost of the wireless sensor are always important factors in the sensor placement scheme. Placement scheme also included the field-tested wireless sensor developed by participating researchers to map spatial distribution of wind and solar energy over the bridge for developing energy harvesters. Following Figure 10 shows locations of all sensors, including AE, accelerometer, strain, string pot and laser sensors on our pilot bridge testing site, the I-270 over Middlebrook Road Bridge in Maryland.

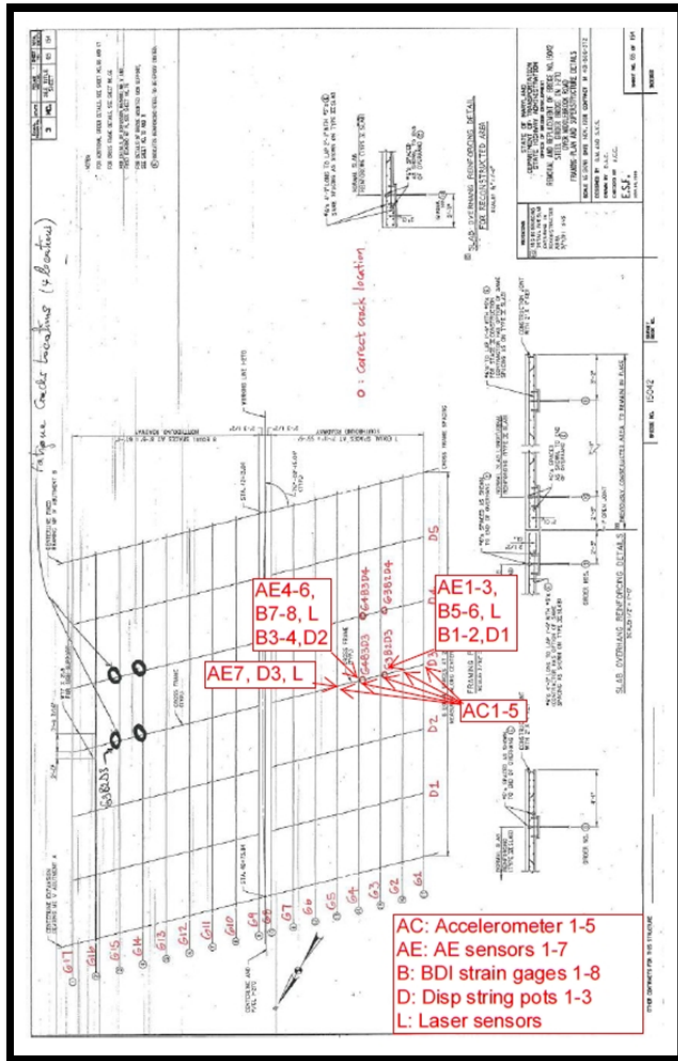


Figure10 - Sensor Locations on MD I-270 over Middlebrook Road Bridge

2.3 Task 1.3: Environmental variable data collection

In order to provide data to support the design of self-contained wireless sensor devices, the following environmental variable data were collected: frequency bands of EMI noise, temperature, moisture, solar intensity and wind speed for developing the miniature wind turbine. Environmental data were collected in the previously defined “preliminary bridge testing” on two sites, one at Paint Branch Bridge on US Route 1 in the State of Maryland and one at NC Beaufort County Bridge in the State of North Carolina (Figure 11).



Figure 11 - Sensor Placement on NC Beaufort County Bridge

3.0 Task 2: Fabrication and characterization of piezo paint AE sensor with reconfigurable sensing dots

The UMD team led this research task on the development of a flexible, reconfigurable, and high-fidelity piezo paint AE (acoustic Emission) sensor (shown in Figure 14 and also a close-up shown in Figure 1) for curved structural surface application. The piezo paint sensor inherits the low-profile and wideband features of the existing piezo paint AE sensor while extending to reconfigurable design that can be assembled into sensor array and be integrated with wireless sensor nodes.

3.1 Task 2.1: Development of flexible piezo paint with great sensitivity

This subtask is comprised of paint formulation, micromechanics modeling, fabrication technique for large area sheets of piezo paint, polarization technique for large area paint, and experimental characterization of paint property (dielectric, elastic, and piezoelectric constants).

Major work conducted includes:

- (1) New design of piezo paint AE sensors were fabricated by an external flexible circuit manufacturer – Tramont and sensor performance was examined in lab in March and April 2012; Additional 40-dB and 45-dB preamplifiers were made in UMD lab to accommodate these piezo film AE sensors both for lab and field tests. Calibration test involving glass capillary breakage and pencil break test were conducted to characterize the broadband performance of piezo film AE sensors.
- (2) Fatigue test frame and full-scale tube specimens were installed in our lab (see Figure 12). This test frame and specimens were used for full scale characterization of piezo paint AE sensor.

-
- (3) Experimental test of a frequency-shift-based crack source location algorithm was conducted on the calibration setup and other steel plates with a 1-inch thickness [Zhou and Zhang 2014a in Table 2 publication list]. This near-field AE monitoring strategy has the advantage of improved representation of crack source information [Zhou and Zhang 2014b in Table 2 publication list].
 - (4) A Labview-based virtual instrument software for data acquisition of piezo film AE sensor data was enhanced by adding new functionalities including automatic link to database and remote sensing ability.

Piezo paint AE sensor with new pattern to maximize frequency shift caused by fatigue crack growth was tested in the steel welded tube specimens in lab, as shown in Figure 12. Piezo paint based AE sensors were installed on the steel tube specimens as shown in Figures 13 and 14. Seven piezo film AE sensors were installed on each specimen to monitor any AE signal caused by fatigue crack initiation and propagation. Five specimens were tested and the average fatigue life is found to be 600k cycles under a stress range of 22 ksi, which is comparable to the stress level observed on the connection plate of the field test bridge in Maryland.

Piezo film AE sensor was validated in the lab with more extensive tests to characterize its performance including steel plates of different thickness that are commonly seen on bridge structures. Bench-top test involving glass capillary breakage and pencil break were conducted to characterize the broadband performance of piezo film AE sensors as well as the attenuation effect of plastic substrate layer on AE signals [Zhou 2013 in Table 2 publication list]. Further experimental test of a frequency shift based crack source location algorithm and Rayleigh wave attenuation relationship based crack source localization method were conducted using both the

field test data and the AE data collected from the steel tube fatigue test. It was also found that flexible piezo paint AE sensor worked well on curved steel tube specimens while piezoelectric ceramic (PZT) discs broke when bonding the sensor to the tube surface.



Figure 12 - Test setup for fatigue testing of full-scale steel tube from traffic signal post

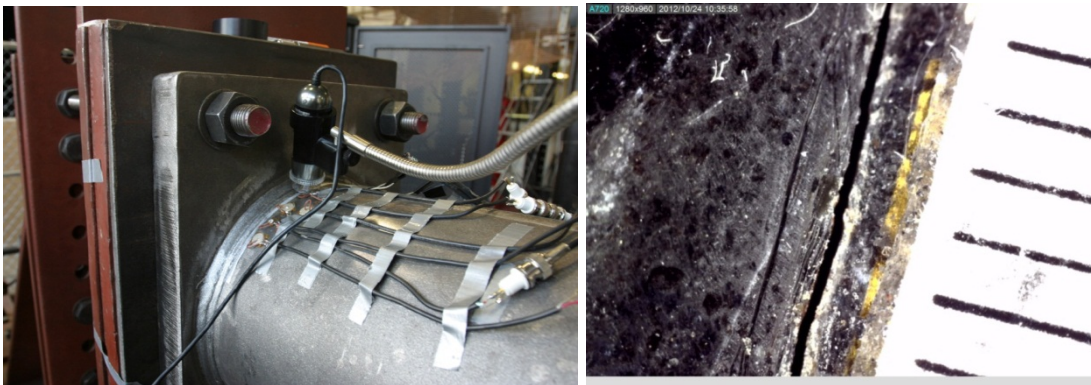


Figure 13 - Digital microscope used for measuring fatigue crack size and growth (left) and pictures of fatigue crack taken using digital microscope (magnification x50)

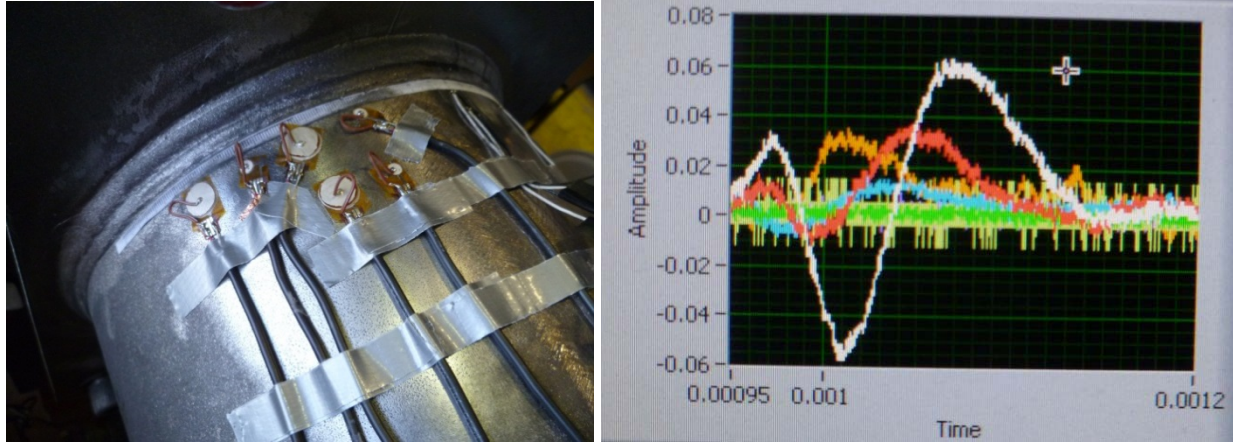


Figure 14 - Piezo film AE sensor (left) and AE signals triggered by fatigue crack growth

3.2 Task 2.2: Development of reconfigurable piezo paint sensor dots (RPPS-dots)

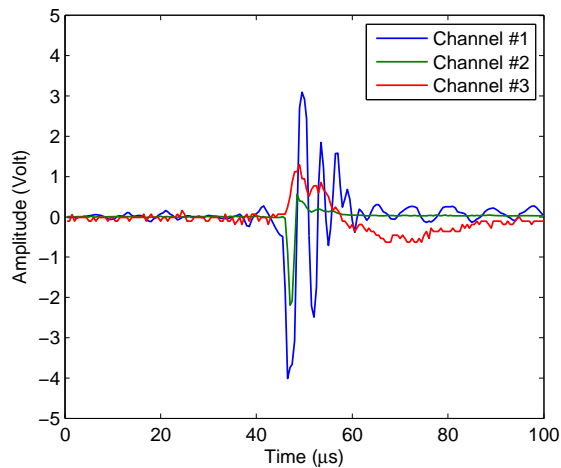
This subtask involves the design and modeling, prototyping and characterization of piezo paint AE sensor, as well as sensor packaging for long-term durability in the field. The reconfigurable sensing dot layer is made of a bondable polyimide film with sub-layers fulfilling different functions: adhesive layer that bond this piezo paint sensor dots to structural surface; electrode sub-layer connecting data acquisition system to the piezo paint sensing element; electro-magnetic shielding sub-layer; and a protective layer that protects the paint sensor from environment effect and thus ensures its durability. Multiple piezo paint sensor dots can be bonded to the structural surface (e.g., steel plate surface near fatigue crack or composite repair patch) into desired sensor dot array pattern. In this design, the base layer is a bondable polyimide film that can be glued to any structural surface. The reconfigurable piezo paint sensor dot array fabricated with this strategy has been tested in lab for their ultrasonic sensing characteristics.

Long-term remote acoustic emission monitoring of the existing fatigue cracks has been carried out on the I-270 Middlebrook Bridge near Germantown, Maryland, in the second year of the project. Meaningful AE data that suggests the existing fatigue crack (as shown in Figure 15(a)) is

active and may be further propagating was collected from long term monitoring. Close examination of these three signals shown in Figure 15(b) reveals that some phase shift occurs between the signals, suggesting this AE event must be induced by near-field source. Figure 16 shows the average frequency spectra of the triggered AE signals of these three piezoelectric film AE sensors. 92 AE signals similar to those shown in Figure 15(b) were used for this averaging. It is seen that there is an attenuation of 8 dB from Channel #1 signal to Channel #2 signal. Considering this attenuation relationship reflected in the measured AE signals, it is believed that the AE signals were triggered by AE activities associated with fatigue crack. This finding has been published in a journal paper [Zhou and Zhang 2014a in Table 2 publication list].



(a)



(b)

Figure 15 - (a) Three piezoelectric film AE sensor near fatigue crack tip on the connection plate; (b) Typical AE signal measured by the three piezoelectric AE sensors.

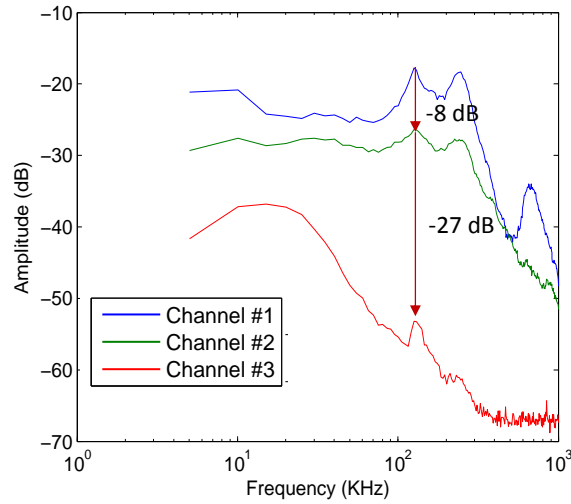


Figure 16 - Average frequency spectrum of triggered AE signals by three piezoelectric film AE sensors

During the field tests in late May 2013 on the I-270 Middlebrook Bridge, some aging issues (humidity and electrode peel off) were identified with several existing piezo film AE sensors and they were replaced with new sensors. In order to protect the new sensors from humidity, a layer of polyurethane coating was applied on top of the sensors for additional protection as shown in Figure 17.

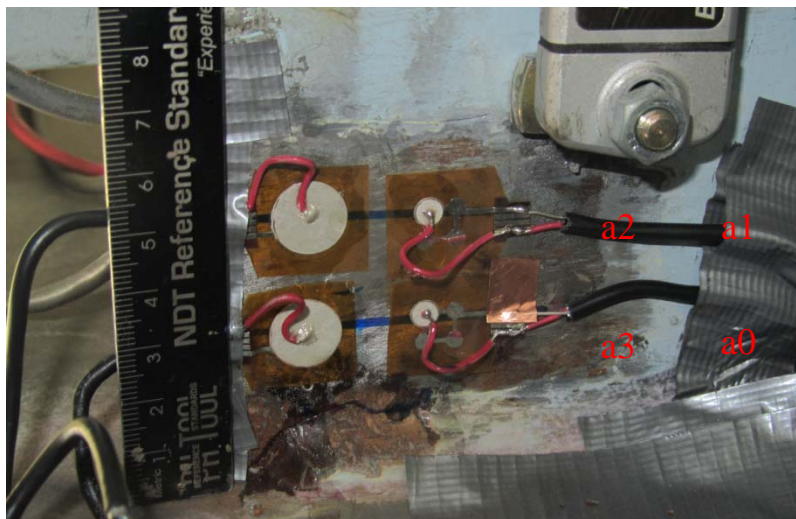


Figure 17 - Newly installed sensor near the fatigue crack (a layer of polyurethane coating was applied on the sensors for extra protection of humidity).

During this field test, the UMD team did pencil lead break tests for calibration purpose. The test set up is shown in Figure 18. Figure 19(a) & (b) show the signals and their frequency spectra, respectively, due to a pencil lead break event captured by all the five sensors including the guard sensor. It can be seen that the guard sensor has nearly no response since it's far away from the simulated source.

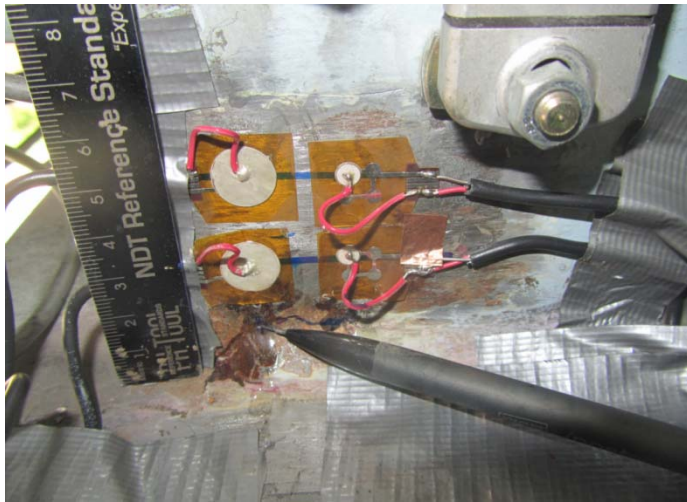


Figure 18 - Pencil lead break test at the middle point of the fatigue crack

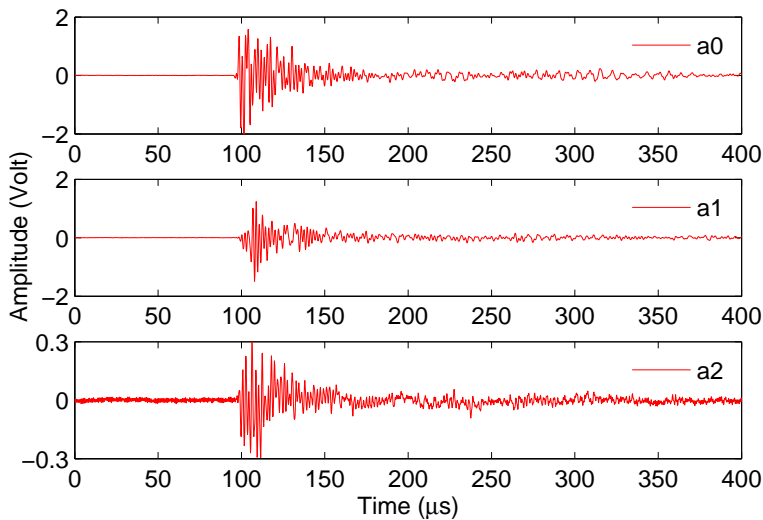


Figure 19(a) - Typical AE signals measured by the three piezoelectric film AE sensors due to pencil lead break

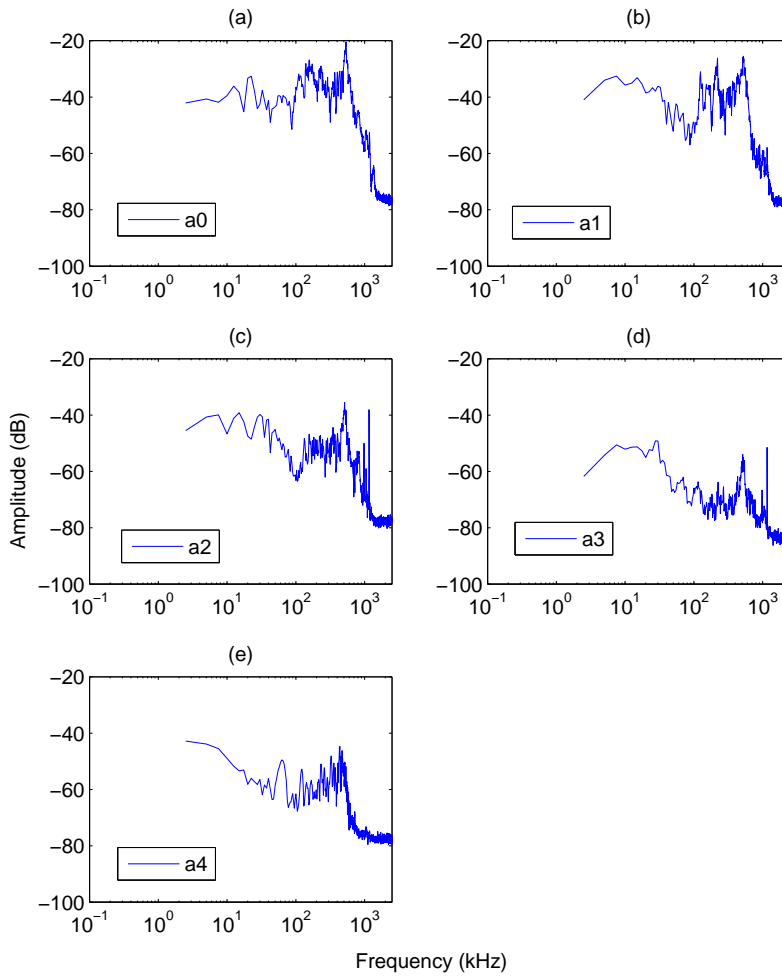


Figure 19(b) - Pencil lead break test conducted at the crack tip (averaged from 40 sets of data)

Channel 0 sensor is connected to the wireless sensor node as shown below in Figure 20(a). Pencil lead break tests were carried out and traffic induced signals were captured. Figure 20(b) shows the status of wireless sensor storing captured signal. Figure 20(c) shows the base station for receiving signals at the abutment. This base station was connected to PXI through USB. The full tests of AE sensors under the lab and field conditions were accomplished under this task.



Figure 20(a) - System set up overview with the wireless sensor

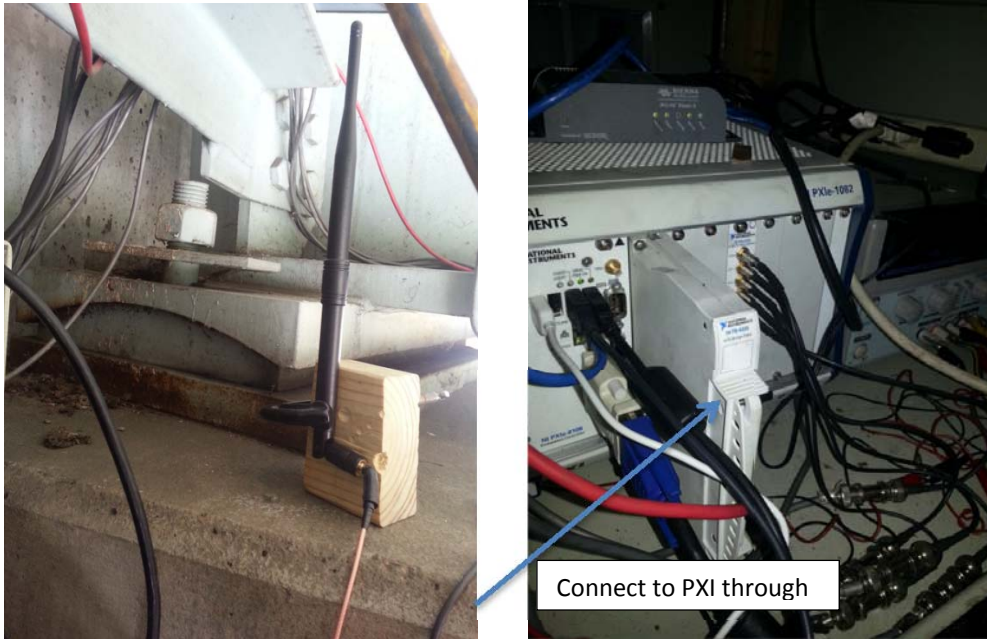


Figure 20(b) and (c) - Wireless sensor receiver at the abutment: (b) base station (c) connection to PXI with USB.

4.0 Tasks 3 & 4: Development of a wireless smart sensor with a hybrid-mode energy harvester and embedded time-reversal (T-R) algorithms

Task 3 was conducted by the NCSU team in two phases. The first phase began with verification of the algorithm to be embedded in the wireless sensor for detecting, locating, and characterizing the AE source. Then a laboratory test was performed to identify and characterize the AE source using the T-R method. The complete work in this task was merged to Task 4 so these two tasks were combined.

Initial promises shown in Thrust area 2 demonstrated that the AE source can be characterized by T-R method through finite element method where the geometry and material properties are required. As the frequency content of the AE source is often wide banded, the T-R procedure could be mathematically approximated by a very simple form: $G(\omega)\bar{G}(\omega)$ where G is the Fourier transformed sensor signals; that is, the sensor signal representing Green's function between the source and a given sensor in the frequency domain. Instead of performing costly physical experiments, a virtual T-R procedure was proposed, If successful, such scheme can be implemented in the wireless sensor by simply calculating $G(\omega)\bar{G}(\omega)$ using the recorded AE sensor signals. Different time windows were performed to choose the minimum duration. For locating the AE source from multiple sensors, the T-R method optimally focuses back to the AE source and retrieves the actual loading function and amplitude. In this subtask, the same numerical simulated sensor data was used for the optimal focusing to verify this approach. The goal of this subtask is to refocus the AE source without knowing the geometry and material properties of the plate.

Laboratory tests of T-R method was performed before field tests. The test structures were pre-cut and placed on a testing machine under loading representative of the normal operation of bridges. The AE source signals were first received by the high-sensitive commercial AE sensors and physically time-reversed and re-emitted back into the structure. The location of AE source using the T-R technique was compared with the triangulation method after removing the dispersion. For entire loading process until failure, a series of AE events can be captured and traced. Since different damage mechanisms reveal different transient wave forms. Significant features of a signal are classified or assigned into different signal classes. A statistical analysis such as Mahalanobis distance classifier was adopted for classifying the damage mechanisms and damage evolution.

Integration of the T-R method with wireless sensors for on-board diagnostics and field test is discussed below.

In Task 4, an integrated wireless smart sensor system including a self-sustained wireless smart sensor, a hybrid-mode energy harvester and embedded diagnosis algorithms was developed. First, a continuous acoustic emission (AE) listening module was developed on the existing platform to extract knowledge from piezoelectric paint sensors and enable appropriate interfacing. Upon its verification and performance evaluation, a new smart sensor was designed and developed. The existing hardware platform and software codes were migrated and extended to the new design. The hybrid-mode energy harvester was derived through improving current prototypes simultaneously. At the final stage, high-speed, multi-channel data acquisition functions were integrated into the FPGA and Microcontroller in the smart sensor and

embedded diagnosis algorithms were designed, evaluated and optimized in conjunction with the results obtained from the system.

4.1 Task 4.1: Continuous low power AE listening capability for wireless sensors with piezoelectric paint sensors

To sense minute ultrasonic signals for AE events, this subtask is to develop a low-power high-gain amplifier up to 60 dB for interfacing the existing sensor platform with the piezoelectric paint sensors. In addition, compensation for environmental factors, such as varying temperatures and ambient noises, needs to be taken into consideration to ensure obtaining physically meaningful signals.

A low-power cascaded compensation topology along with stages of charge/differential/ voltage amplifiers is used to interface with the piezoelectric paint sensors to provide signal conditioning and amplification. An initial design effort has been conducted by the participating researchers before the start of the project; during the project the strict requirement of high dynamic range and power efficiency in real-world applications pushes for verification and further optimization on linearity, drift and thermal stability. Notably the nature of re-configurability of the paint sensor dots calls for a flexible and extendable design to be compatible with multiple sensors. Initial tests were performed on the existing prototypes of paint sensors to verify dynamic ranges, sensitivity and power consumption.

Work accomplished in this subtask is summarized as follows:

- 1) Designed and tested the new high-speed, multi-channel wireless piezoelectric sensor board.
- 2) Modified the enclosure to install the new sensor board and battery (Figure 21).

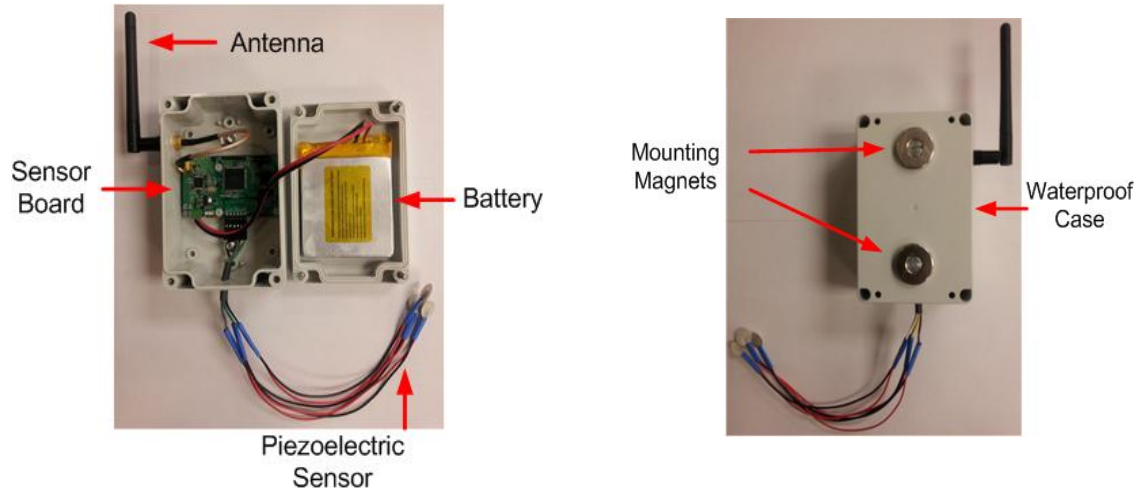


Figure 21- The new enclosure of the piezoelectric senso

3) Redesigned the piezoelectric amplifier circuit for better signal reception (Figure 22).

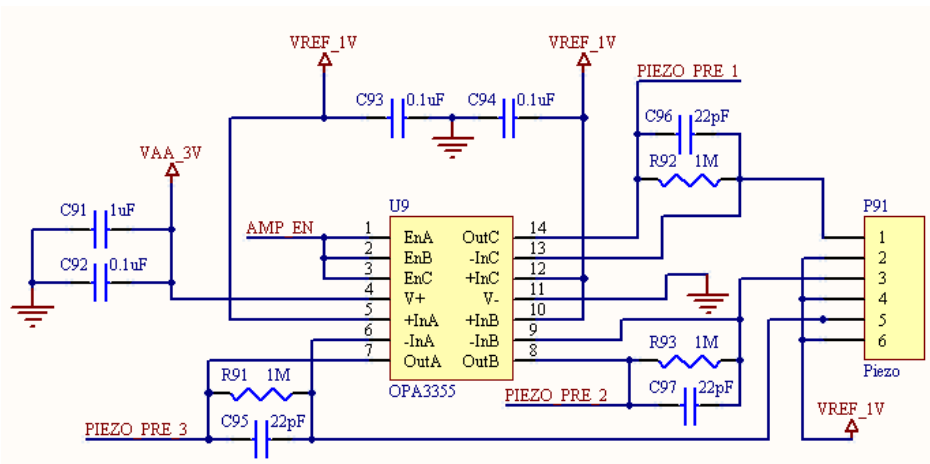


Figure 22 - The new design amplifier circuit of the piezoelectric sensor

4) Finished the piezoelectric acquisition program of the microcontroller and FPGA (Figure 23).

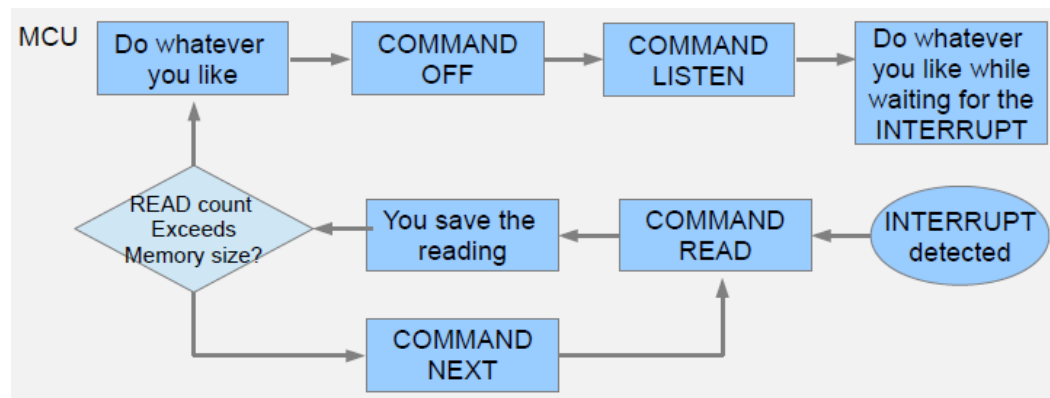


Figure 23 - The scheme of the MCU program

5) Tested the wireless piezoelectric sensor in the lab (Figures 24 and 25).

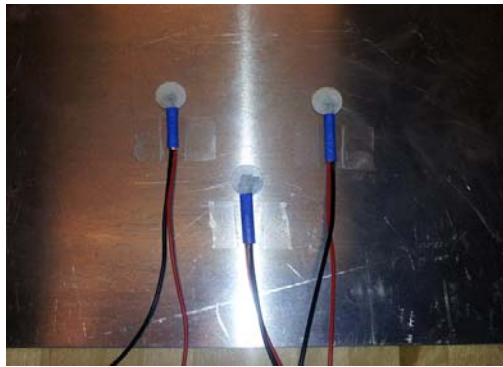


Figure 24 - The test platform

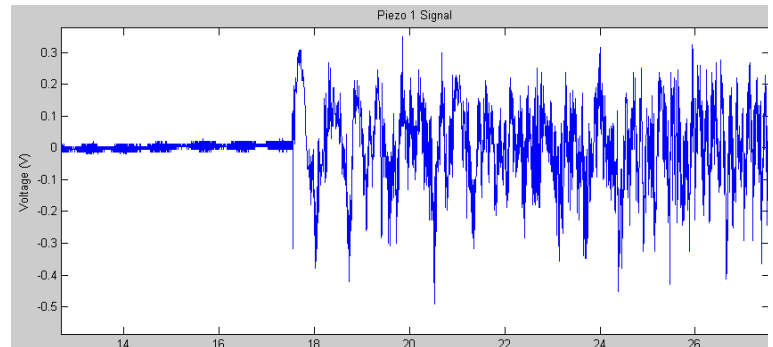


Figure 25 - The test result

5.2 Task 4.2: A hybrid-mode energy harvester with MWTS and solar panel

The major part of the hybrid-mode energy harvester is a miniature wind turbine system (MWTS). Due to time-varying wind speed, solar panels molded onto the exterior of the MWTS were also included as an auxiliary supply to increase energy density and supplement the instantaneous current limit. The harvester basically serves as a charger for the flexible battery integrated in the smart sensor to provide continuously charging currents and compensate its self-discharging losses.

The hybrid harvester was designed, optimized, and fabricated in this subtask. The system design comprises: (1) the design of the harvester itself and, (2) that of the supporting electronic circuits. For the electronic circuit design, the circuit by the participating researcher was optimized to increase conversion efficiency and maximize power transfer from the harvester.

The MWTS is composed of miniature turbine blades, gear box, and mechanical electrical generator. The NACA 4412 and NACA 4422 profiles were used as the baselines for designing the blades. The 3-D blade geometry was optimized to maximize the lift-to-drag ratio using finite element software (ANSYS CFX). The number of blades was also considered to obtain proper tip speed ratio and starting torque. The blades were fabricated through the compression molding

process. An electrical generator for transmitting the power was selected and optimally matches the performance.

The newly-engineered thin-film flexible solar panel was wrapped around the completed MWTS to serve as supplement supplies. It is predicted that 50 mW/cm³ can be achieved in the dark and higher numbers are anticipated in lighted condition. Laboratory tests were at last carried out by assembling the harvester in a nozzle to evaluate output powers under various conditions.

Achievements of this subtask include:

- 1) Enhanced and evaluated wind turbine energy harvester - A miniature wind turbine (MWT) for energy harvest have been manufactured and tested under the resistive loads from 10 Ω to 461 Ω at the wind speeds of 2, 2.5, 3, 3.5, 4 and 4.5 m/s, as shown in Figure 26. The sample output voltages obtained from experiments is shown in Figure 27.

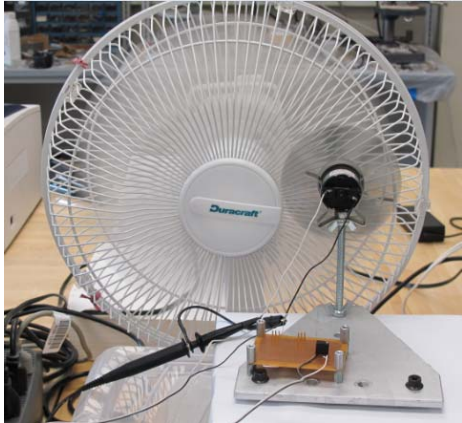


Figure 26 - Test photo of the MWT

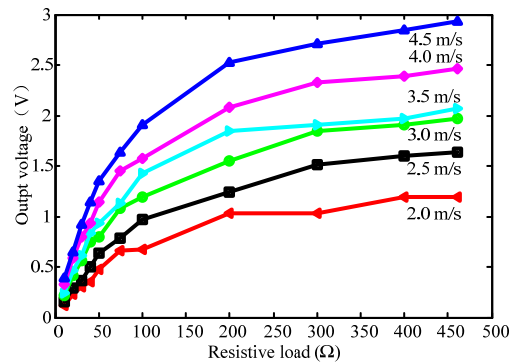


Figure 27 - Tested output voltage of the MWT

- 2) Developed and evaluated a new Buck-Boost Converter - A new Buck-Boost Converter has been designed for storing the energy extracted from the wind energy. The values of various elements in this boost converter have also been determined. The effectiveness of the Buck-Boost Converter has been verified.
- 3) Installed and tested Energy Harvesting System on NC Beaufort County Bridge - A total of seven

wireless sensors were deployed on the bridge and each equipped with an energy harvesting device located at where the sensor was installed. Each of these devices collects both solar power and wind energy for supplying power to the sensor (Figure 28). These sensors are located at 1/2 span, a quarter of span and the support.

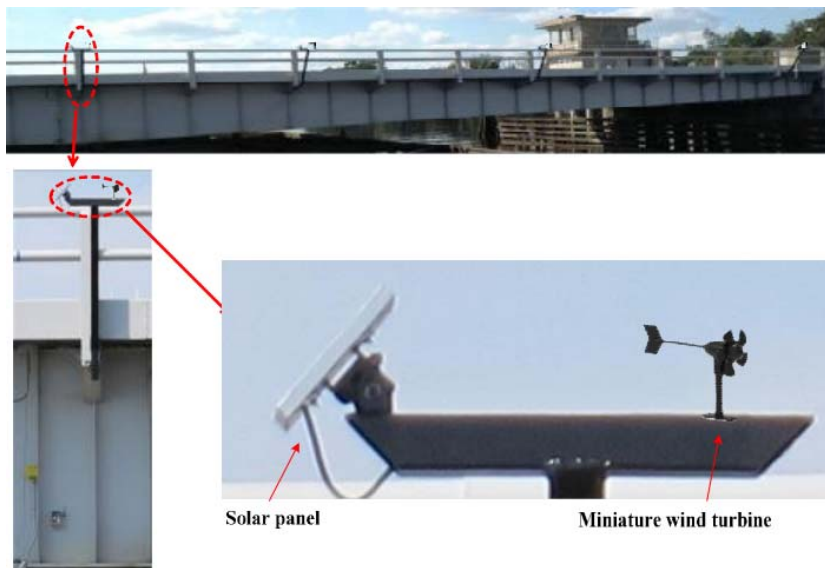


Figure 28 - Energy harvesting devices

5.3 Task 4.3: Mathematical cores in FPGA and embedded algorithms

It has been noted that the parallel architecture employing multiple processors/controllers and hardware-assisted approaches can enhance the efficiency and significantly lower the total system power consumption. No dedicated DSP is available in COTS for the diagnostic algorithms. While FPGA provides an excellent platform for developing and prototyping DSP for specialized applications, the proprietary nature of intelligent property cores impedes the progress of smart sensor development. Therefore, mathematical operation units need to be implemented in the hardware level to significantly improve computational efficiency.

Diagnostic procedures operating on continuous data and complex algorithms require further investigation on efficient utilization of the computational modules as well as on partial conclusions from Task 3 (T-R method). Embedded algorithms were then developed to minimize the amount of data traffic. Simulated data was used as input for comparison purpose. The instantaneous current consumption and execution time were monitored and recorded to analyze power profile. Methods to further improve power efficiency were planned and implemented.

Work accomplished in this subtask is summarized as follows:

- 1) Soldered the redesigned wireless piezoelectric sensor board and test it with power (Figure 29).



Figure 29 - The Redesigned Wireless Piezoelectric Sensor

- 2) Debugged the piezoelectric acquisition program of the microcontroller and FPGA.
- 3) Conducted pencil lead break experiments with new wireless piezoelectric sensor in the Lab (Figures 30 & 31).

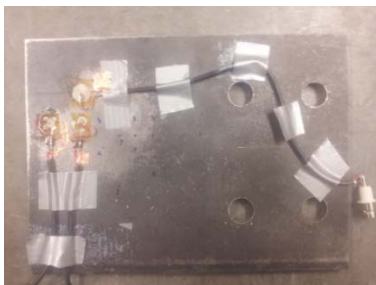


Figure 30 - Test Platform

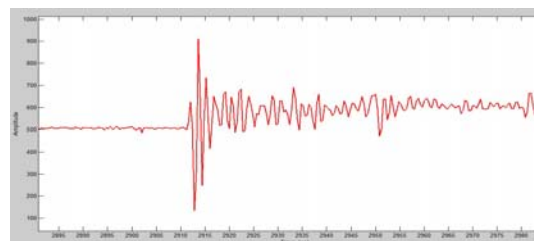


Figure 31 – Sample Pencil Lead Break Test

5.0 Task 5: Developing ISHM in both laboratory and field environments and implementation with Bridge Management System

Testing of the prototype ISHM system in controlled laboratory environment enables us to investigate (validate and evaluate) and reveal the interplay between key system parameters and system performance, which is usually considered an indispensable step for technology validation and debugging before field implementation. Clearly, field testing in a real-world setting provides a comprehensive assessment of the ISHM performance under various environmental interferences.

5.1 Task 5.1: Developing ISHM for bridges in controlled lab environment

Lab test involves implementation and performance characterization of the prototype ISHM system on bridge elements including steel plate components with fatigue details and bolted connections subject to fatigue loading. In order to demonstrate the ISHM for fatigue crack localization, a specimen comprised of 1-inch thick steel plate with welded stiffener was fabricated and cyclically loaded to generate fatigue crack near the tip of welded stiffener. The test specimen is comprised of four ASTM A36 steel plates: 1" thick plate, ¼" thick longitudinal stiffener and transverse stiffeners. Stiffeners were welded to the 1"-thick plate with 3/16" fillet weld. The 1" plate is considered to be thick enough for Rayleigh wave to develop in the plate so that the sensor couple theory for AE source localization is applicable. The target is detecting and monitoring fatigue cracks at early stage. This was done using proper hardware and signal processing algorithms. More sophisticated moment tensor based filter design was applied to enhance the crack detection ability. A picture of the fatigue test setup including the specimen and loading head of the servo-hydraulic actuator is shown in Figure 32(a). The specimen is

anchored to a loading frame with two steel plate and bolts. The specimen is cyclically loaded as a cantilever beam with a load range of 0.26 to 2.76 kips at a loading frequency of 1.5 Hz. Four piezoelectric film strain sensors (denoted as a0 and a1) were bonded to the test specimen. Sensor a0 and a1 are 25 mm and 40 mm away from the weld tip respectively. Fatigue crack was first seen at the weld tip location at load cycle number $N=170,000$ cycles. A close-up view of the fatigue crack is shown in Figure 32(b). Figure 32(c) shows typical AE signals captured by the two AE sensors after fatigue crack was seen in the test specimen. The corresponding frequency spectra are shown in Figure 32(d). The primary tasks of lab testing of the ISHM system consist of AE signal recoding de-noising, damage localization, and data analysis works such as reliability updating and remaining life estimation. A scaled version of ISHM was installed on structural test specimens for ISHM system prototyping and validation (Figure 32).

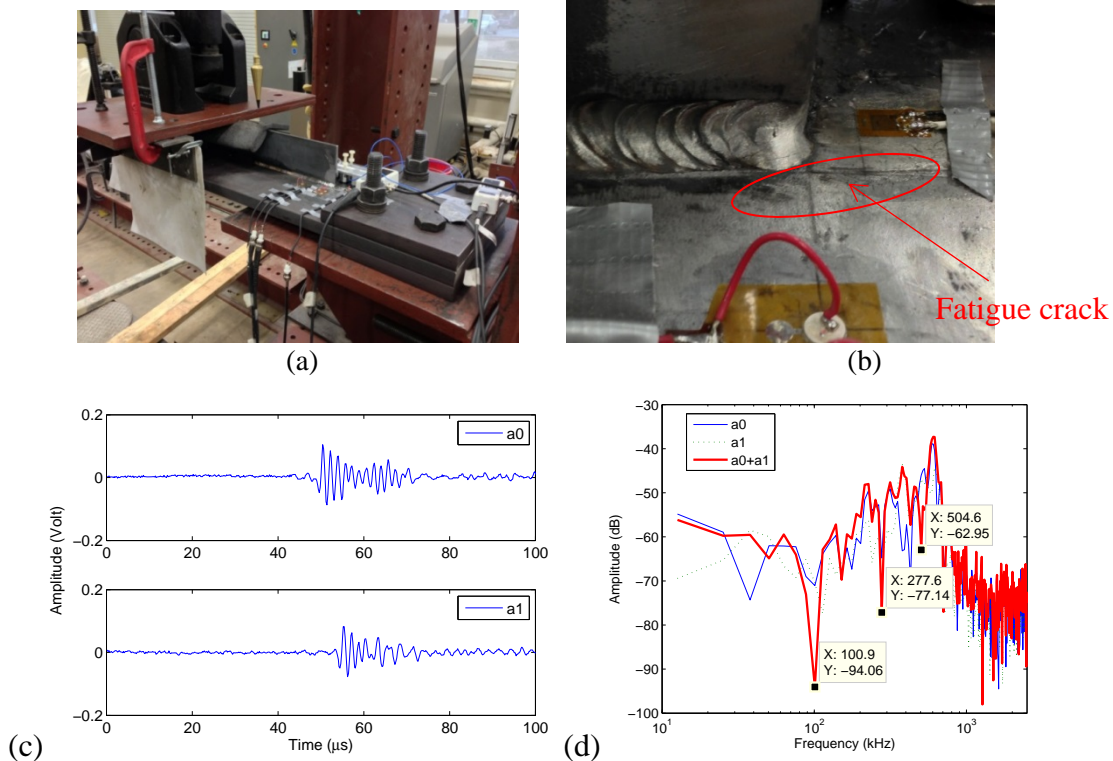


Figure 32 - Fatigue test of welded plate specimen and AE monitoring: (a) test setup; (b) Close-up view of fatigue crack near longitudinal stiffener weld toe at load cycle number $N =182,000$ cycles; at load cycle number $N =185,300$ cycles: (c) signals of sensor a0 and a1; (d) frequency spectra of the sensor couple signal (a0+a1)

The lab tests of ISHM involve:

- 1) Test the noise signal of the piezoelectric sensor in the lab (Figure 33).

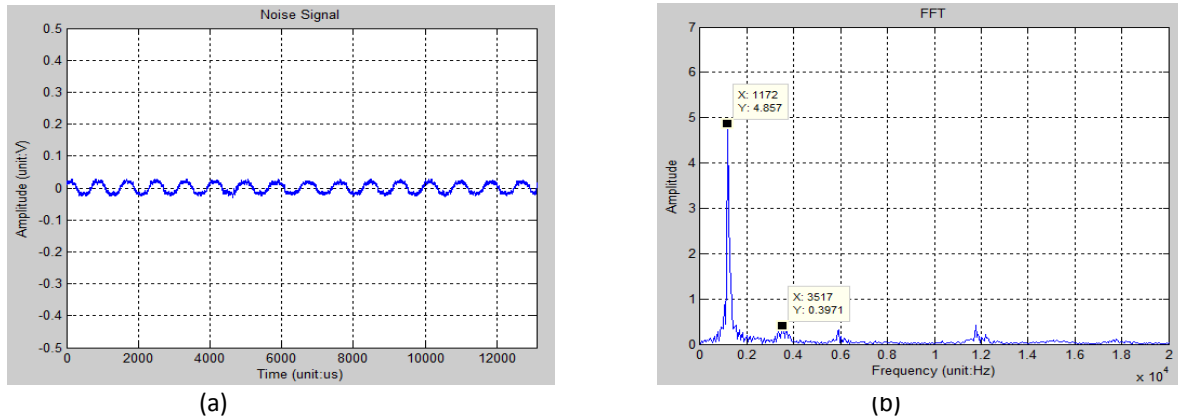


Figure 33 – (a) Noise signal waveform (Set 1) and (b) FFT of noise signal (Set 1)

- 2) Optimize and redesign the software structure of the wireless piezoelectric sensor.

5.2 Task 5.2: Demonstration of ISHM system for bridges in field environment

The ISHM system requires intensive investigation in real-world operating conditions before final commercialization. Field implementation on bridges includes design of wireless sensor placement scheme, finite element analysis, performing the test, and data analysis including diagnostics of the monitored structural elements. Field tests were performed in the following full-scale bridge structures: one medium-span steel girder bridge (I-270 over Middlebrook Road Bridge), and one long-span steel bridge (I-95 over Pautuxent River Bridge) within the MDSA bridge system. Attention has been given to possible complications such as noise levels, environmental conditions, and wireless sensor placement when performing field test of ISHM for autonomous on-line diagnosis of the integrity of civil structures.

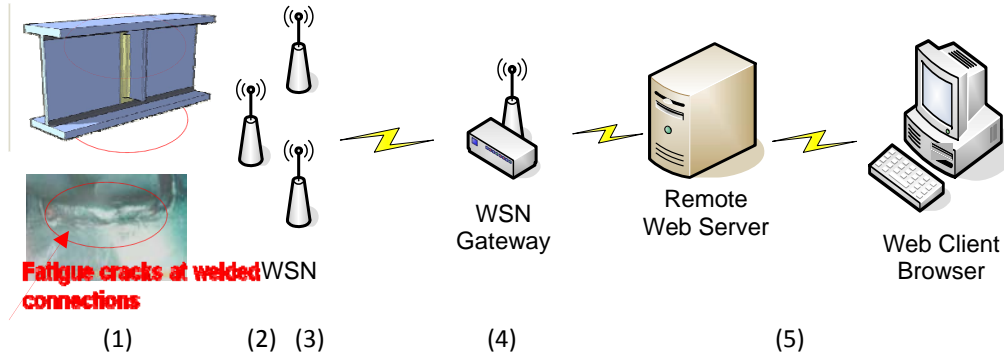


Figure 34 - Remote Wireless Bridge Monitoring System

Figure 34 shows the schematics of the ISHM system with remote sensing ability: (1) wireless sensor nodes including AE sensors, strain gages, thermocouples, etc., (2) Wireless Smart Sensor Network with (3) Energy Harvester, (4) Data Acquisition System (DAQ), with Wireless Communication Modem, and (5) Web-based Remote Data Processing and Data Storage for application (Zhang, Zhou, Fu and Zhou, E. 2013; Fu, Zhao, Saad, Zhang and Zhou 2014.) Field tests have been conducted on I-270 over Middlebrook Road Bridge and I-95 NB over Patuxent River.

5.2.1 Field tests and Finite element Analyses on I-270 over Middlebrook Road Bridge

(A) Field tests

Crack locations and sensor placement on the framing plan are shown in Figure 10 of this report. Types of sensors used in this project are: 1. piezoelectric paint AE sensors; 2. wireless accelerometers; 3. laser sensor; 4. ultrasonic distance sensors; 5. BDI strain transducers; and 6. String pots. Figures 35 and 36 show the crack on Girder 3 and their respective sensor locations.

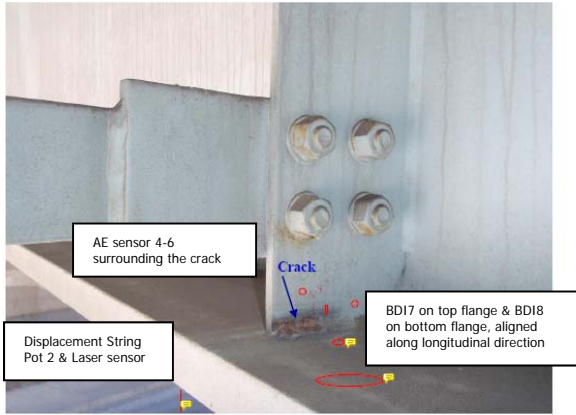


Figure 35 - Crack at G4B3D3 (Girder 4 Bay 3 Diaphragm 3) and sensor locations

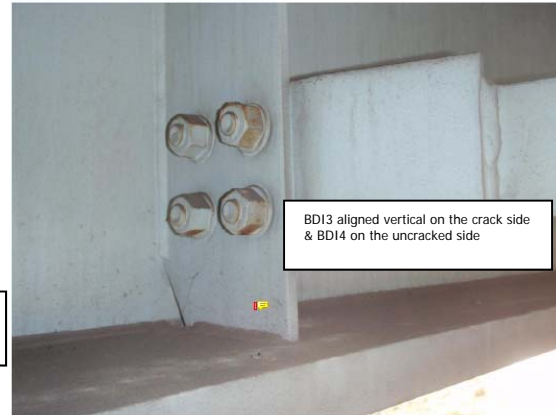


Figure 36 - No Sign of Cracking at G4B4D3 (Girder 3 Bay 4 Diaphragm 3) and one sensor

A total of seven AE sensors were installed on Girder 3 and Girder 4. Three piezoelectric paint AE sensors were installed on Girder 4. Two of them were placed on the cracked connection plate (see Figure 37) while the third was placed on the uncracked connection plate to provide ambient noise AE data (Figure 38). Figure 39 shows the installation of those AE sensors. Same arrangement is for Girder 3.

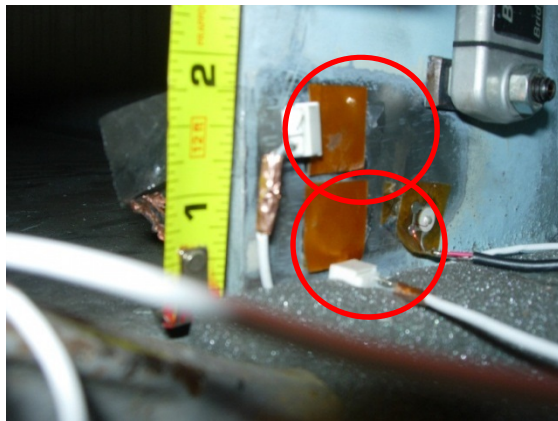


Figure 37 - Piezoelectric paint AE sensor on cracked connection plate (red circled, for monitoring fatigue crack in the weld between the connection plate and lower flange)



Figure 38 - Piezoelectric paint AE sensor (blue circled, for monitoring ambient noise since there is no fatigue crack on this side connection plate)

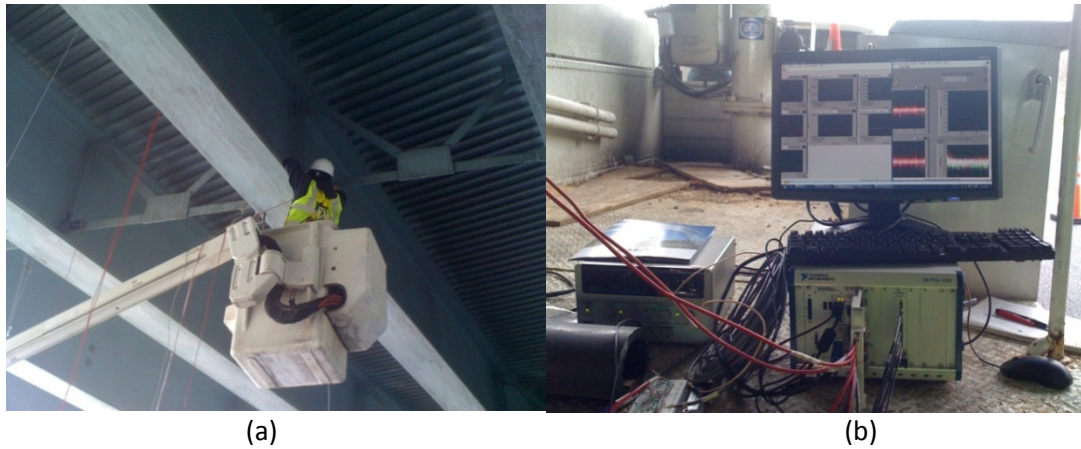
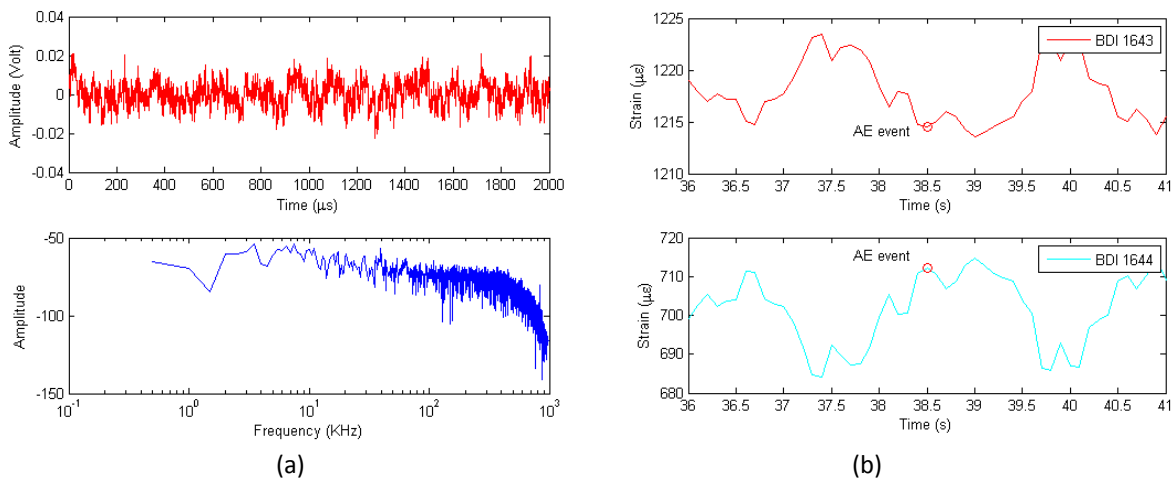
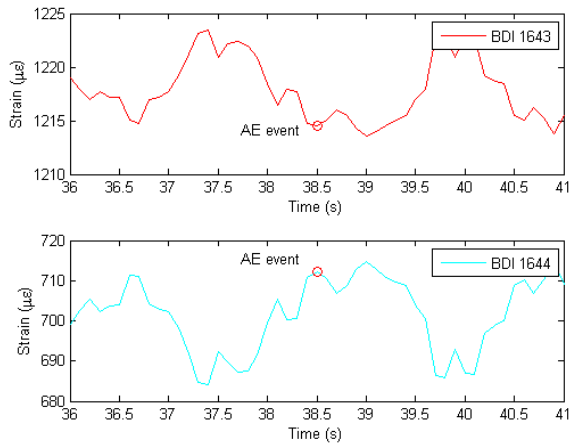


Figure 39 - (a) Installing AE sensors and wiring; (b) AE data acquisition

Over this field test period on March 20 and 21, 2012, no fatigue-crack-related AE signal was observed. Samples of AE data and their frequency characteristics (by applying FFT on time series data) are shown in Figure 40. Some AE signals related to fatigue crack growth were detected later during longer monitoring periods. For more than two AE sensors, the synchronized signals can be used for AE source quantification using the T-R method.





(c)

Figure 40 – Sampled AE data collected by piezo paint AE sensor on Girder 4: (a) ch4 AE data on cracked connection plate; (b) ch6 AE data on uncracked connection plate ; (c) corresponding strain data (from BDI strain gage near ch4 AE sensor)

(B) Finite Element Analyses (FEA)

For investigating the fatigue performance of the bridge and the diagnosis/prognosis purpose, several three-dimensional (3D) finite element models were developed by CSiBridge for linear-elastic structural analyses. The concrete deck, eight I-girders, and connection plates connecting diaphragms and girder webs, were modeled by shell elements, while all the diaphragms were modeled by truss elements. Boundary conditions represented actual characteristics of supports where the translations of x-, y-, z-directions are fixed at the abutments. In order to locate the hot spot, a specific global model refined meshed around the hot spots was built for analysis with detailed view of this global model is presented in Figures 41 and 42.

To validate our FE model, experimental data from the field test and numerical results from CSiBridge were used for comparison. In the numerical study too find the natural frequencies, the bridge was subjected to dead load only. The first modal frequencies obtained from our FE model to field study are 3.22 and 3.245 Hz, respectively, which are considered close in comparison.

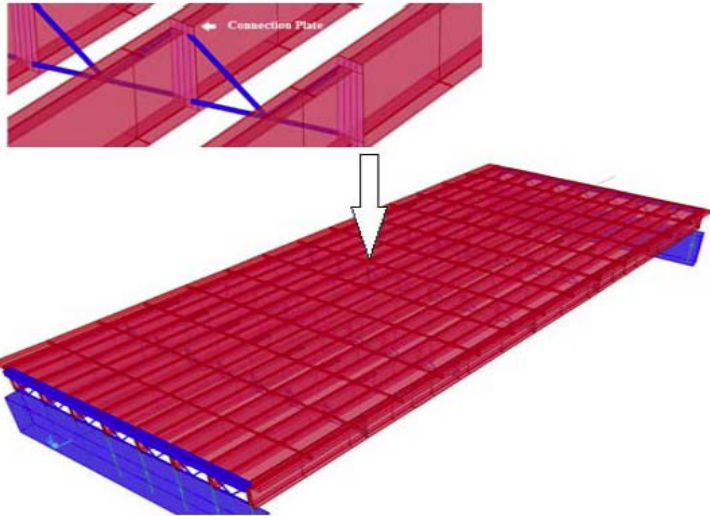


Figure 41 - Finite Element Model

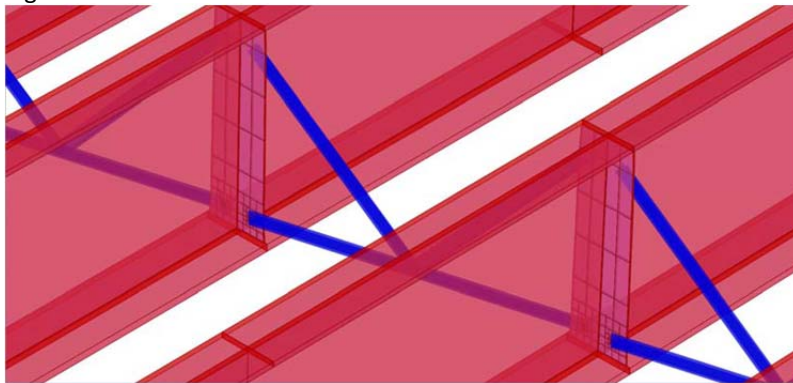


Figure 42 - Close-up View of Refined Portion of FEM without Deck Elements Shown

Figure 43 shows the displacement time history of midpoints at the bottom flange for Girder 3 and Girder 4. The maximum differential displacement is 0.08 in under 10-min simulated truck loading.

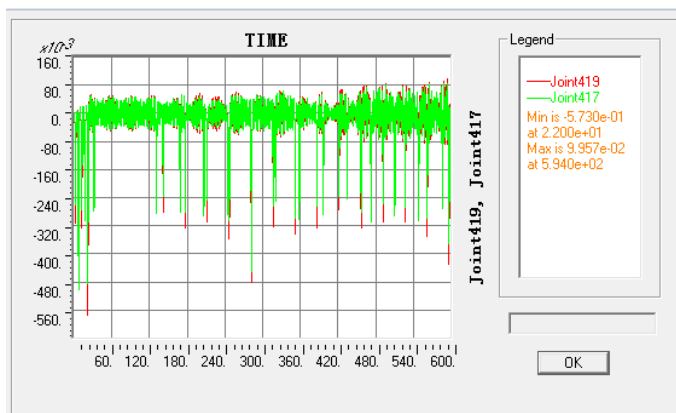


Figure 43 - Midpoint displacements for G3 (Joint 419) and G4 (Joint 417) under 10-min truck loading, unit - inches

To check the hot spots where BDI strain transducers were placed, Figure 44 shows the time history curves of two hot spots of the connection plate, located at Girder 3 Diaphragm 3. Shell element 252 is on the G3crack side, and shell element 250 is on G3 uncrack side. Both of them are on the same face. The maximum tension stress is 17.86 ksi, and the maximum compression stress is 11.79 ksi under 10-min truck loading. This also suggests that the fatigue crack at this location may be active.

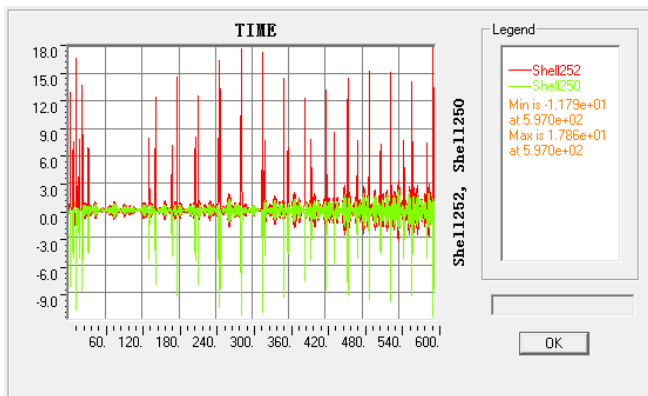


Figure 44 - Stress of Hot Spot (Shell252-G3crack side, shell250-G3uncrack side), unit-ksi

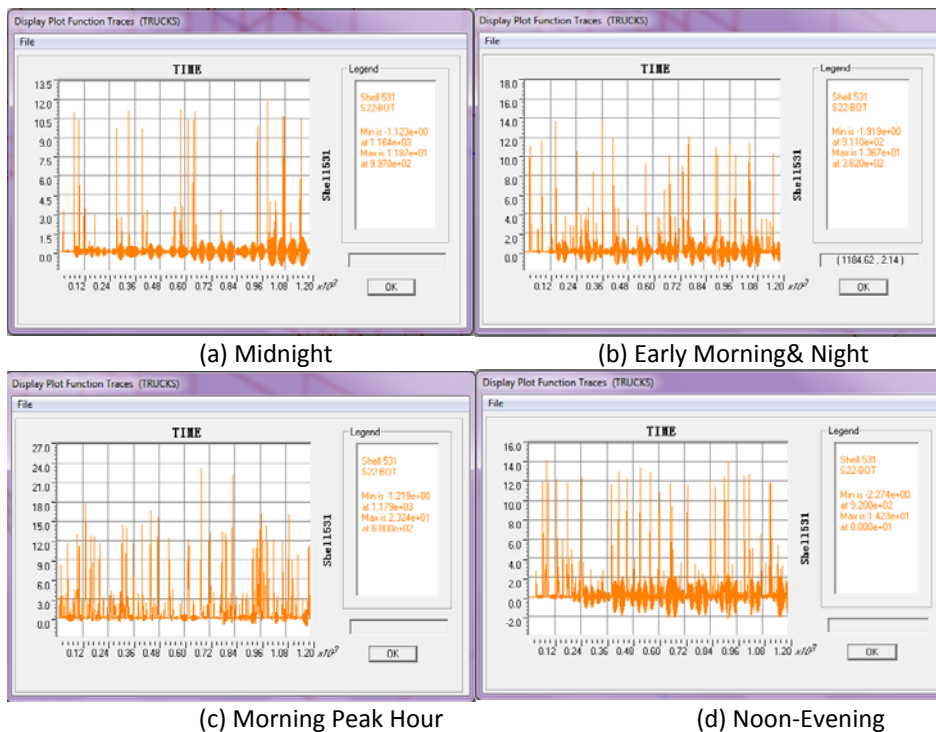


Figure 45 - 20-min Time History Results of Stresses on the Connection Plates of Girder 3 Diaphragm 3 during Four Time Periods

Using the simulated truck loading, four load cases were defined, where each of them corresponded to a specific time period of one weekday. In each load case, truck loadings were applied on the bridge deck, passing through the bridge in the simulated patterns. After the structural analysis corresponded to that load case, the time-history curves of concerned details under truck flow were obtained. Figure 45 shows four time history curves of one hot spot of the connection plate, located at Girder 3 Diaphragm 3 where BDI strain transducers were placed. Shell element 531 is on the G3 crack side with the maximum tension stress is 23.24ksi and the maximum compression stress is 2.274ksi during one weekday.

Figures 46 and 47 show the stress contours of Girder 3 and Girder 4 at different times when the stress of hot spots reached their maximum values, respectively. The stress of connection plates was much higher than that of the bottom flange based on both the long-term monitoring and numerical simulation. Hot spot is at the weld connection. The results of finite element modeling matched well with what has been observed in the field.

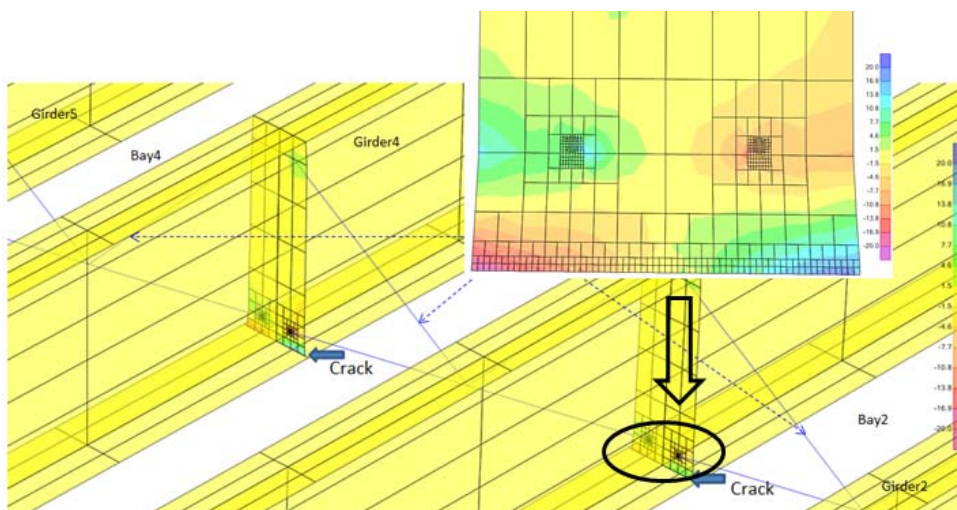


Figure 46 - Zoom-in Stress Contour of Connection Plate (Girder 3 Diaphragm 3) at T=597second during Morning Peak Hour

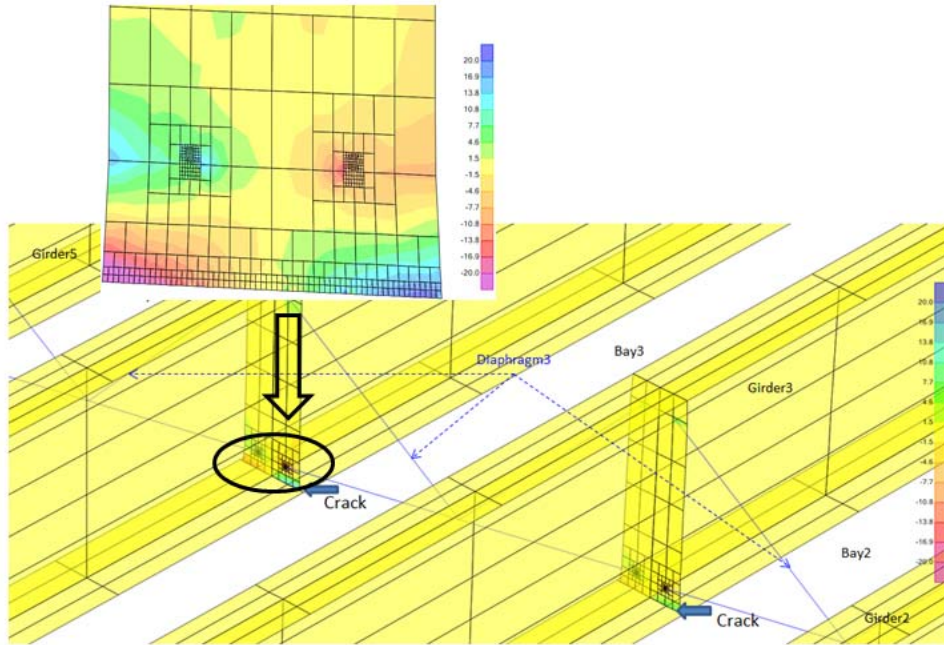


Figure 47 - Zoom-in Stress Contour of Connection Plate (Girder 4 Diaphragm 3) at T=283 second during Morning Peak Hour

5.2.2 Field tests and Finite element Analyses on I-95 NB over Patuxent River

(A) Field tests

The location and the longitudinal view of the bridge are shown in Figure 48. Wireless AE Sensor (Left) and the corresponding crack to detect are shown on the left and right, respectively, of Figure 49. Solar Panel and Wind Turbine for sensor energy harvesting are mounted on the bridge and shown on the left and right, respectively, of Figure 50. Figure 51 shows two big solar panels are deployed for powering the base station and the small solar panel and the fan combination on the far side are for the wireless sensors.



Figure 48 - I-95 NB Bridge Over Patuxent River



Figure 49 - Wireless AE Sensor (Left) and Crack (Right)



Figure 50 - Solar Panel (Left) and Wind Turbine (Right)



Figure 51 – Big and Small Solar Panels

Field test of the piezo film acoustic emission sensors was carried out on the I-95 Bridge. Four piezo film AE sensors were surface mounted at locations near the existing fatigue cracks. The waveforms of AE signals acquired by these piezo film AE sensors and wireless sensor nodes show significant lower frequency contents but lacked higher frequency content (from 100 kHz to 300 kHz) typically associated with fatigue crack propagation. This observation confirmed the engineers' speculation with monitoring data, that is, the existing fatigue is inactive, and most likely the acquired AE signals were due to fracture surface rubbing and friction. Laser distance sensors were used to measure bridge girder deflection of Girder #2 and Girder #3 (girders where fatigue cracks were monitored). The locations of the girders where deflections were measured were approximately 48'-10" from the south bridge abutment. Peak displacement of 5 mm and 6 mm were recorded for Girder #2 and Girder #3 respectively during a 1-hour recording for each of these two girders.

Two field tests, one for preliminary test and one for the final and demo test, by using wireless AE sensors were conducted on March 12th to 14th and on May 20th to 22nd. During the first test, we got seven times triggered signal on March 12th and twelve times on March 14th (Figure 52).

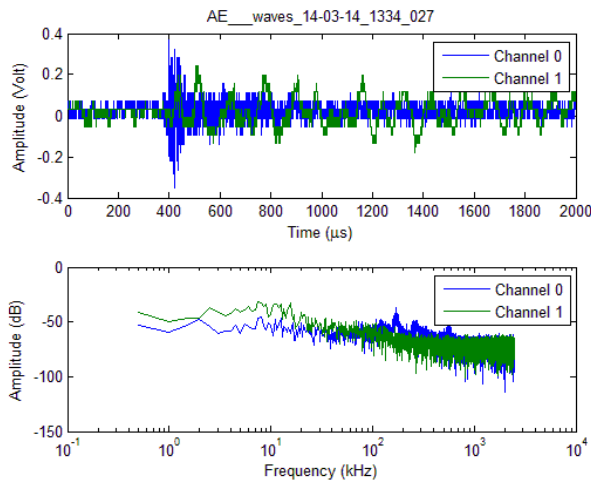


Figure 52 - Acoustic emission signal recorded by the piezo film AE sensor (channel 0) and commercial wideband AE sensor (HI-1000 by Dunegan Eng) when the notched steel plate test specimen underwent significant deformation

The second test, the demo test, was open to invited guests. Federal, state and local government engineers were invited. Many came for the demonstration and were very impressed with the innovated system (Figure 53).



Figure 53 – Guests from the MD State DOT

(B) Finite Element Analyses (FEA)

Both UMD and URS teams built FEA models based on software packages CSiBridge and LUSAS, respectively. LUSAS results are shown here to diagnose the stress ranges that would have caused the fatigue cracks.

As depicted in Figures 54 and 55, the FEM by LUSAS includes one half (four girders) of the eight-girder, three-span continuous superstructure due to symmetry about the centerline of roadway. Boundary conditions for symmetrical deformation (restrained only for lateral translation and rotation about the longitudinal axis) were defined at all the nodes along the longitudinal vertical plane of symmetry. Fixed girder bearings at the piers were represented by translational restraints in the vertical and longitudinal directions. Expansion girder bearings at the abutments were represented by translational restraints in the vertical direction. Lateral restraints were added only to the exterior girder supports at the abutments and piers.

The FEM used thick shell elements for the deck and spatial frame elements for all the cross frame and lateral bracing members. The main girders were modeled with a combination of spatial frame and shell elements. For the majority of the three-span structure, the girders were modeled with spatial frame elements along their center-of-gravity. Special link members were defined to connect the girder elements with the cross frame and lateral bracing elements at the actual spatial points where these members intersect. A refined portion of the FEM was defined in one end span, as depicted in Figures 55 to 57, where shell elements were used to model all the girder webs and flanges, as well as cross frame connection plates and intermediate stiffeners. The refined portion is 47'-2" long including three consecutive lines of cross frames and served the purpose for stress extractions at the welded connections of interest for this investigation.

The deck shell elements are rigidly connected to the supporting girders throughout the entire model to represent the composite construction. Rigid planes were defined at both ends of the refined portion at the frame element-to-shell element interface for the main girders. Girder-to-deck and girder-to-bearing links were created using spatial frame elements. Girder-to-deck links were created at all stiffener and connection plate locations. All frame elements were positioned along their center-of-gravity and were defined with their respective section and material properties.

The existing, or "as-is", concrete deck was modeled as 8.5" thick shell elements with compressive strength of 3,600 psi based on the proportions of concrete deck strengths and thicknesses. The deck consists of the lower 5.5" of 3,000 psi concrete from the 1971 "as-built" plans and the top 3" of 4,500 psi concrete from the 2001 deck rehabilitation.

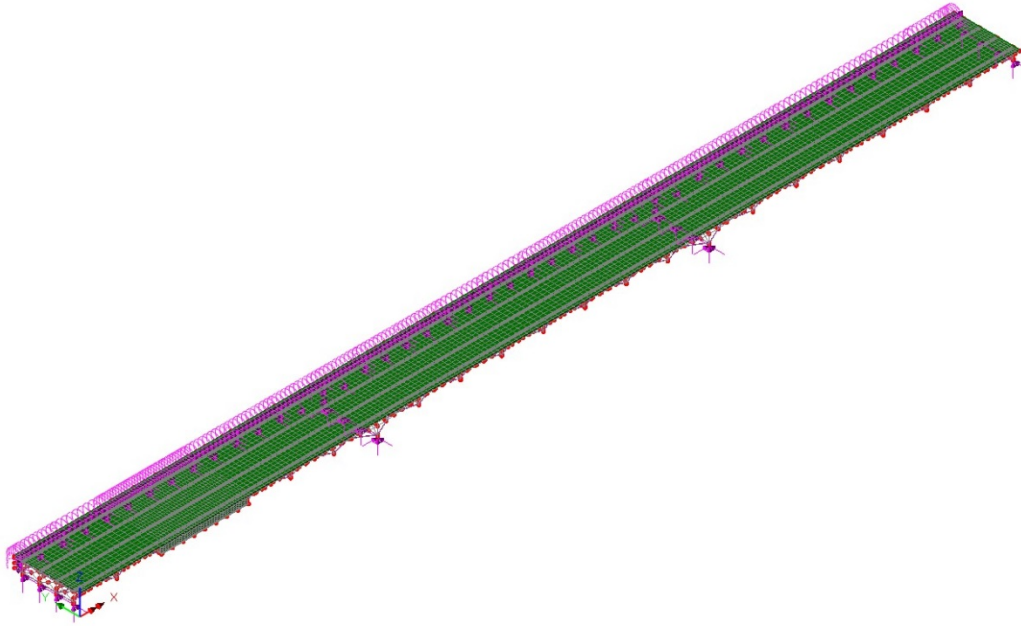


Figure 54 - Isometric View of FEM for One Half of Eight-Girder Three-Span Continuous Structure

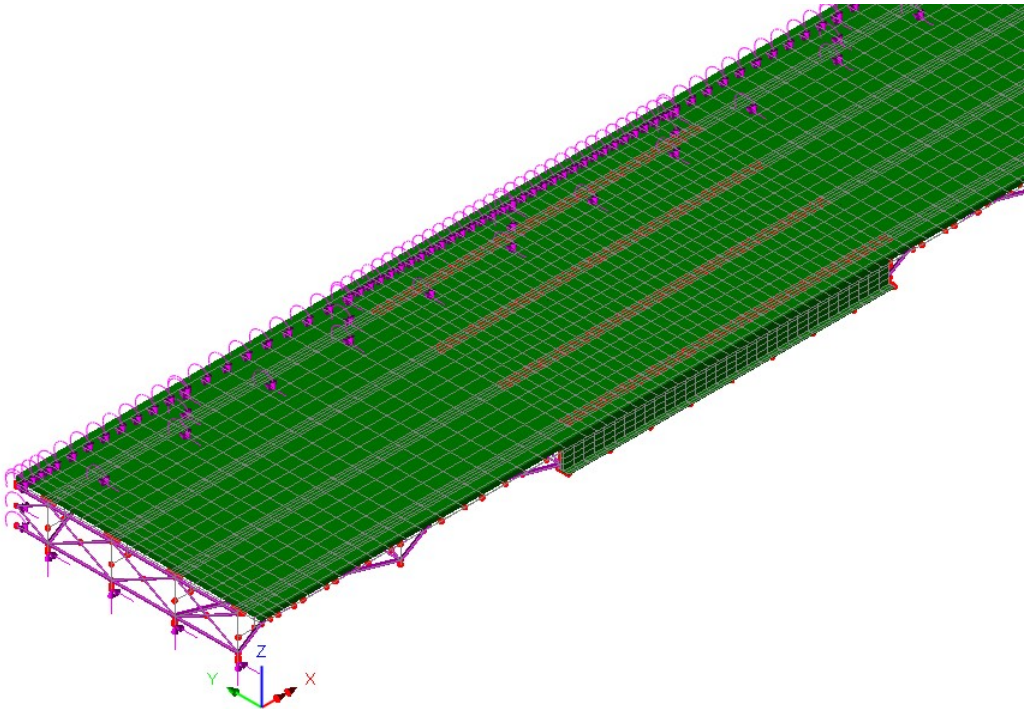


Figure 55 - Isometric View of Refined Portion of FEM with Deck Elements Shown

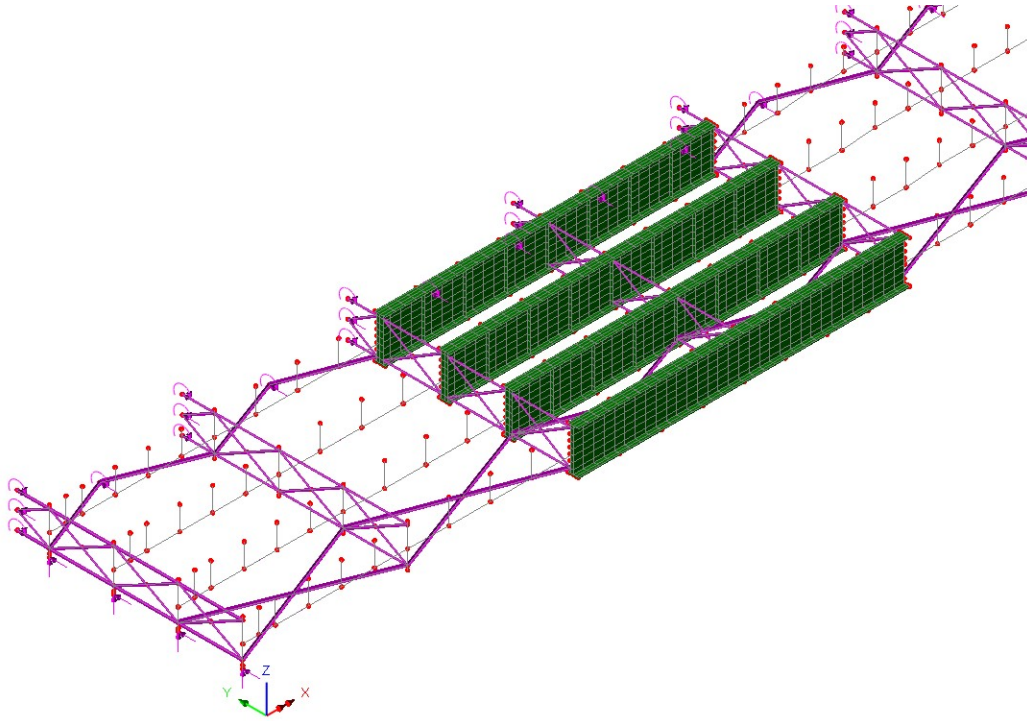


Figure 56 - Isometric View of Refined Portion of FEM without Deck Elements Shown

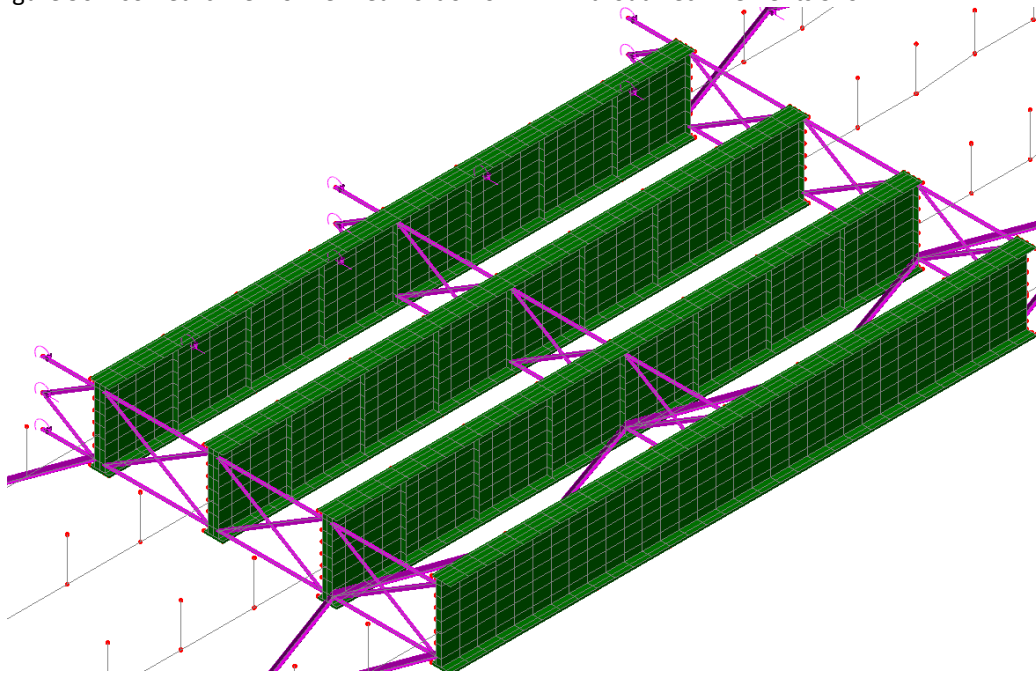


Figure 57 - Close-up View of Refined Portion of FEM without Deck Elements Shown

Possible driving forces for the fatigue cracks would have to be vertical tensile stress, horizontal shear stress, or the principal tensile stress due to their combined actions, along the connection

welds. These stresses are most likely a result of transverse deformations of the deck relative to the girder as indicated in the 1995 report by Greiner Inc. titled “Load Testing and Structural Evaluation, I-95 over Patuxent River Bridge No. 16197”, as illustrated in Figure 58. This investigation focuses on estimating the orders of magnitude of tension in the welded connections due to live load.

Live load induced stresses in the welded connections between the cross frame connection plates and the girder top flanges were extracted along the middle cross frame line in the refined portion of FEM. The live load used in the FEA was the Maryland Type 4 Vehicle of 70,000 lbs gross vehicle weight with three closely spaced rear axles. This vehicle realistically represents the actual dump trucks and is used as a primary load rating vehicle by MD State Highway Administration.

The FEA investigated the local stresses in the welded connection by varying two parameters: (1) lateral position of wheel loads, and (2) deck thickness/stiffness. A total of five different cases were studied as described below and key results summarized in Table 1. For all the five cases analyzed, the longitudinal position of the MD Type 4 Truck remained the same: with its middle rear axle right above the middle cross frame line in the refined portion of FEM, as depicted in Figures 59 to 61. Girders are numbered as G1 through G4 from the exterior to the centerline of the bridge, and S denotes girder spacing.

Case 1 – 8.5” deck thickness with Type 4 Vehicle exterior wheel line at $0.4S$ between G2 and G3

Case 2 – 8.5” deck thickness with Type 4 Vehicle exterior wheel line at $0.5S$ between G2 and G3

Case 3 – 8.5” deck thickness with Type 4 Vehicle exterior wheel line at $0.6S$ between G2 and G3

Case 4 – 8.0” deck thickness with Type 4 Vehicle exterior wheel line at 0.5S between G2 and G3

Case 5 – 9.0” deck thickness with Type 4 Vehicle exterior wheel line at 0.5S between G2 and G3

It should be noted that all the live load cases correspond to simultaneous application of two MD Type 4 Vehicles symmetrically placed about the bridge centerline due to the symmetrical nature of the half model.

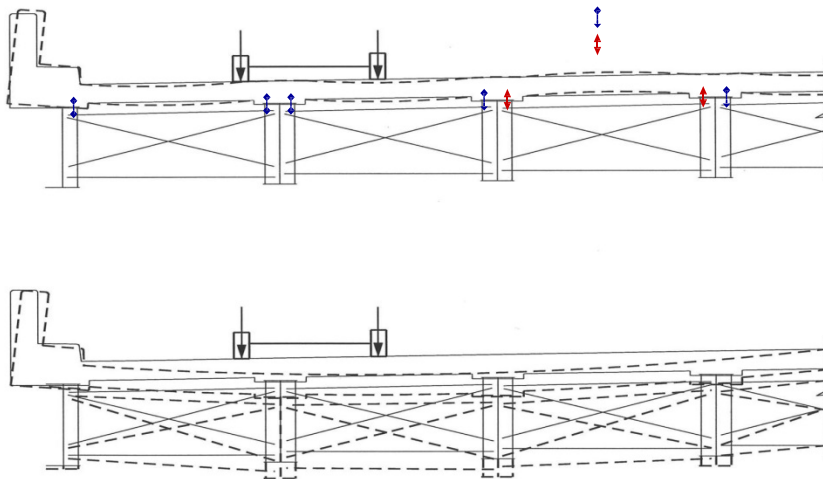


Figure 58 - Illustration of Live Load Induced Deck Deformations as Causes for Tensile Stresses in Cross Frame Connection Plate to Girder Top Flange Connections (from 1995 Greiner Inc. Report)

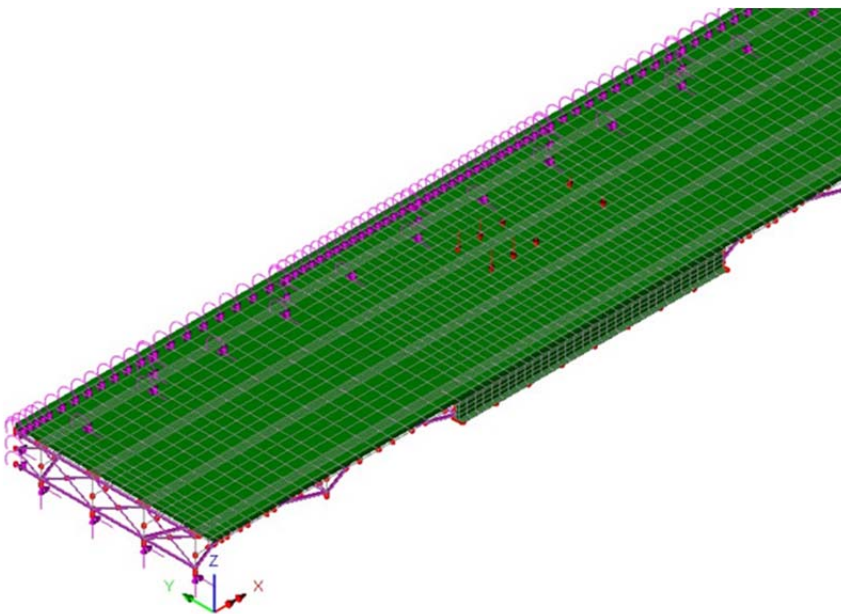


Figure 59 - Illustration of MD Type 4 Vehicle Position in Isometric View – Case 2

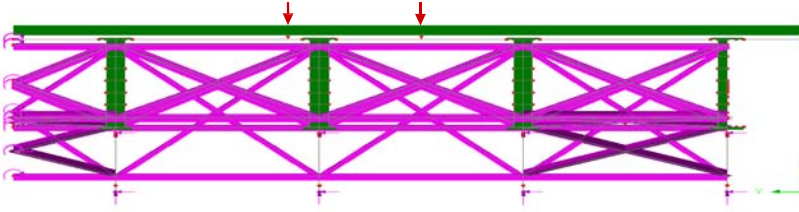


Figure 60 - Illustration of MD Type 4 Vehicle Position in Cross Section View – Case 2

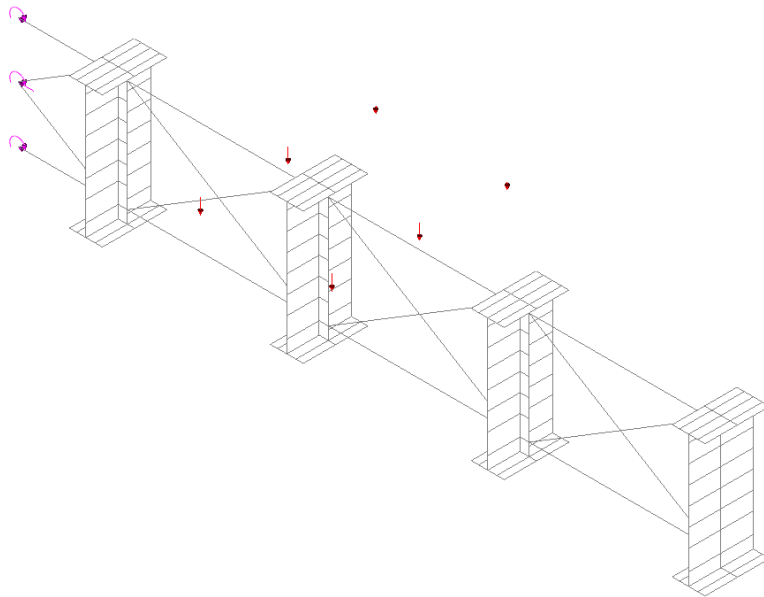


Figure 61 - MD Type 4 Vehicle Position with Middle Cross Frame of Refined Portion of FEM – Case 2

Selected FEA results are presented in Figures 62 to 69.

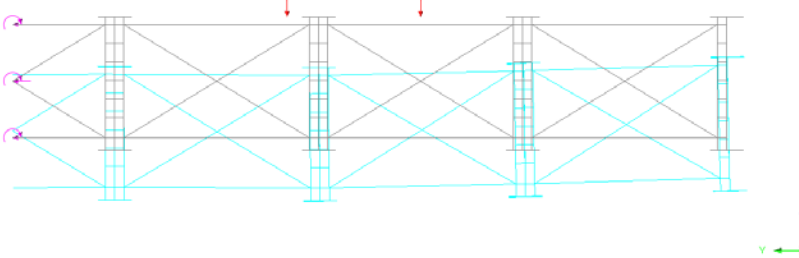


Figure 62 - Deformed Shape of Middle Cross Frame of Refined Portion of FEM – Case 2

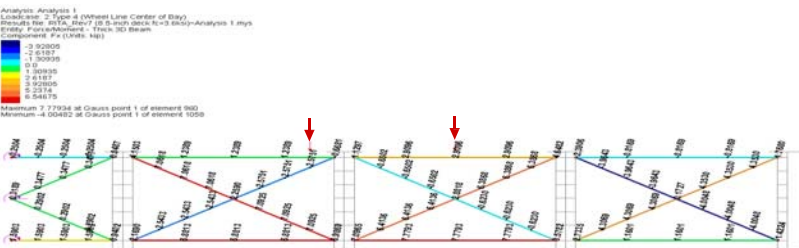


Figure 63 - Axial Member Forces of Middle Cross Frame of Refined Portion of FEM – Case 2

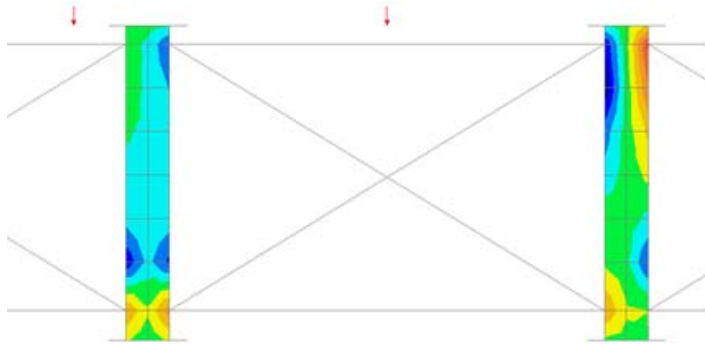


Figure 64 - Vertical Stress SZ Contours in Cross Frame Connection Plates of G2 and G3 at Middle Cross Frame of Refined Portion of FEM – Case 2

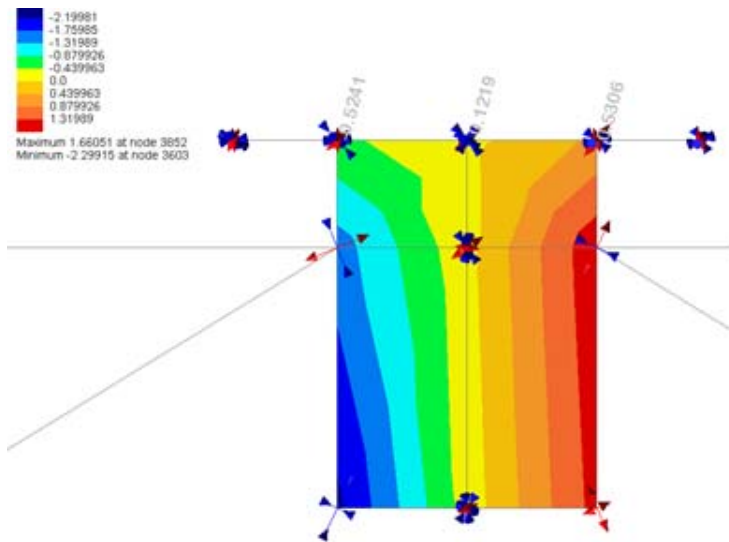


Figure 65 - Close-up View of Vertical Stress SZ Contours in Cross Frame Connection Plates of G2 at Middle Cross Frame of Refined Portion of FEM – Case 2

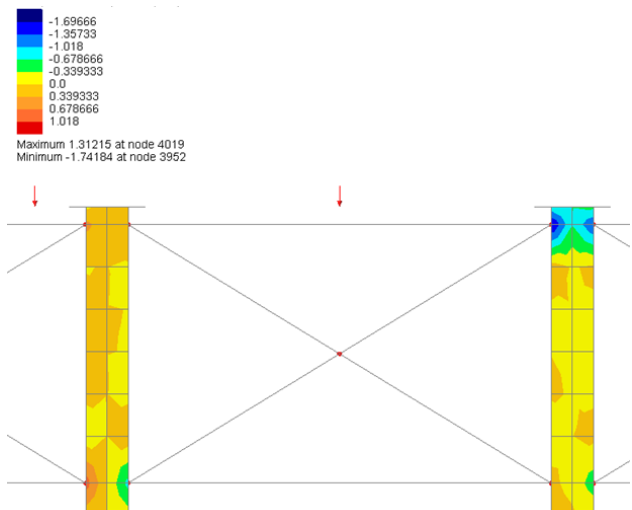


Figure 66 - Shear Stress SYZ Contours in Cross Frame Connection Plates of G2 and G3 at Middle Cross Frame of Refined Portion of FEM – Case 2

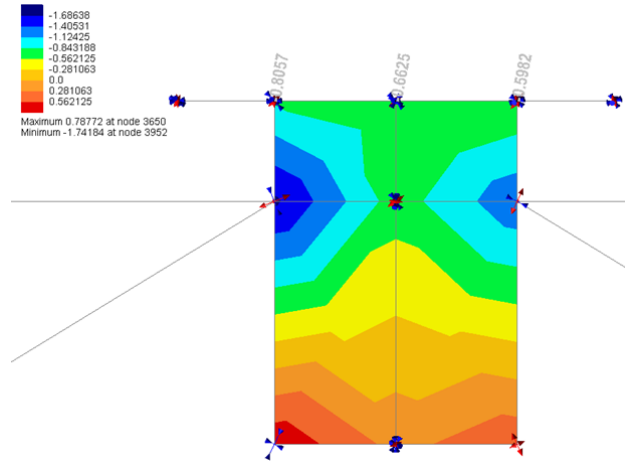


Figure 67 - Close-up View of Shear Stress SYZ Contours in Cross Frame Connection Plates of G2 at Middle Cross Frame of Refined Portion of FEM – Case 2

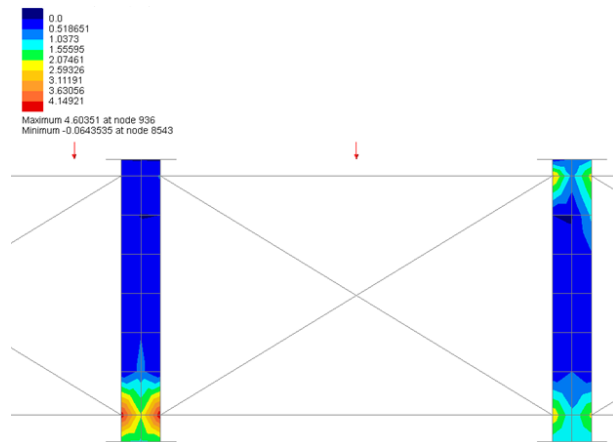


Figure 68 - Principal Stress S1 Contours in Cross Frame Connection Plates of G2 and G3 at Middle Cross Frame of Refined Portion of FEM – Case 2

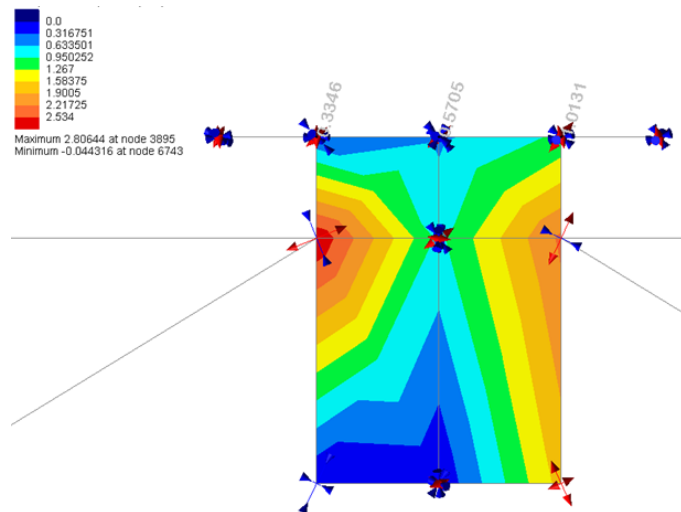


Figure 69 - Close-up View of Principal Stress S1 Contours in Cross Frame Connection Plates of G2 at Middle Cross Frame of Refined Portion of FEM – Case 2

Table 1 – I-95 Bridge Stresses in Cross Frame Plate-to-Girder Top Flange Connections at G2 due to Two Symmetrically Placed MD Type 4 Vehicles without Dynamic Impact

Case No.	Deck Thickness (in)	Wheel Load Lateral Position	Max Vertical Stress SZ		Max Shear Stress SYZ		Max Principal Stress S1	
			(ksi)	%	(ksi)	%	(ksi)	%
1	8.5	@0.4S	0.489	92%	0.774	96%	0.959	95%
2	8.5	@0.5S	0.531	100%	0.806	100%	1.013	100%
3	8.5	@0.6S	0.513	97%	0.789	98%	0.978	97%
4	8.0	@0.5S	0.573	108%	0.848	105%	1.084	107%
5	9.0	@0.5S	0.490	92%	0.765	95%	0.946	93%

The following observations can be made from the limited FEA investigation:

(1) Deformations of bridge deck relative to supporting girders in the bridge cross section can cause vertical tensile stresses in the welded connections between cross frame connection plates and girder top flanges. These stresses are highest at the outer edge of the connection plate where all the existing fatigue cracks on the I-95 over Patuxent River Bridge have initiated from.

(2) Magnitudes of tensile stresses in the connection depend on the magnitudes and positions of wheel loads of crossing vehicle(s). The stresses listed in Table 1 are for illustration purposes and are taken from connection plates at G2 for three different truck positions. There are certainly many live load cases that can produce greater tensile stresses in the connections of concern.

(3) The stresses listed in Table 1 are only tensile stress components due to the MD Type 4 Vehicles Compressive stress components at the same location due to simultaneous or nearly simultaneous vehicles should be of much greater magnitudes, and the resulting stress ranges may be significant for the Category C fatigue detail (LRFD Table 6.6.1.2.3-1 Description 5.4)

(4) A comparison of live load Cases 1, 2, and 3 suggests that a wheel load applied at the center of a bay (0.5S, where S = girder spacing) causes the highest tensile stress in the connection of

concern in the adjacent unloaded bay, compared with wheel load positions at 0.4S and 0.6S in the same bay.

(5) Under the same live load, a thinner deck results in higher tensile stresses in the connection. A comparison of Cases 2, 4 and 5 suggests an increase of 7% in principal tensile stress for a 0.5" reduction in the deck thickness. In fact, the current SHA design standards would require a 9.0" thick deck of 4,500 psi concrete for the 9'-2" girder spacing compared with the existing 8.5" deck of a composite compressive strength of 3,600 psi.

5.3 Task 5.3: Improving quantitative bridge condition assessment in the Bridge Management System (BMS)

The primary method for conventional bridge condition assessment is qualitative based on visual observations. Differences between theoretically calculated and observed life prediction may differ by an order of magnitude. Currently in BMS, the ratings used to describe various possible conditions of a bridge element are neither accurately defined nor linked to the NDE inspection results affecting the element deterioration. The quality of such inspection and condition *rating* practice is thus subjective (visual inspection based on the inspector's view) and time delayed due to inspection cycles (about every two years). The accuracy of these ratings can be improved with the information from structural health monitoring technologies. An improved process to apply condition ratings would include non-destructive evaluation and possibly computational and probabilistic analysis of damage. The flowchart in Figure illustrates the decision process a structure would undergo before applying the FHWA condition rating index.

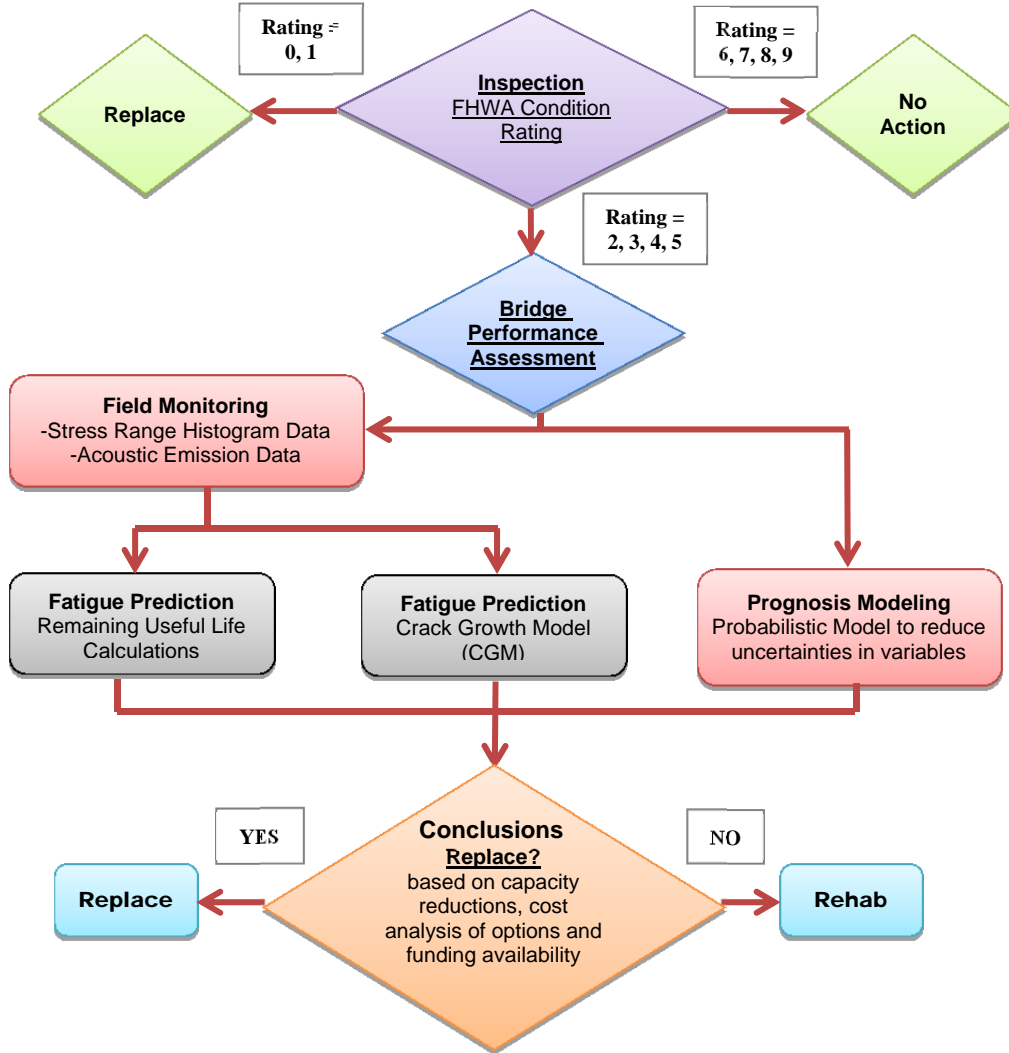


Figure 70 - Flowchart to illustrate improved application of condition ratings

As seen in the first stage of the flowchart, if the structure is thought to be in satisfactory condition or better (ratings = 6, 7, 8, 9), the decision of “No Action” can be made right from the start. Likewise, if the structure is thought to be rated into failure or failed condition (rating = 1, 0), then the structure inarguably needs to be replaced. If the structure is given a rating of 2, 3, 4, or 5, then further analysis is needed. The data acquired from structural health monitoring, fatigue prediction models and remaining useful life calculations can be computed. In parallel,

crack growth models can be used with damage accumulation models as well as probabilistic models to account for uncertainties.

The ISHM integrates two different probabilistic deterioration prediction models - a global Markovian-based model used by current BMS and local probabilistic mechanics based deterioration model driven by continuous monitoring data. The global model identifies the critically damaged structures and forecasts the overall deterioration and required maintenance funds for both short and long term planning for a bridge network or a bridge component while the local probabilistic deterioration model utilize sensor data to quantitatively evaluate the reliability of critical bridge components and their remaining useful life, thus optimize their maintenance. A similar 2-level approach has also been proposed by Lounis and Madant (2002) for bridge management, but their approach didn't take advantage of continuously collected sensor data. The ISHM system is a sensor driven approach which yields multi-dimensional information about the reliability evolution of the monitored bridge structure in future operation years.

5.3.1 Fatigue Predictions, Remaining Useful Life

For structural components subjected to cyclical loading their performance is commonly characterized by an S-N curve. S-N curves are obtained from constant amplitude fatigue tests performed on samples of the material at different stress levels. The curves are derived from plotting the tested nominal stress amplitudes (S) against the number of cycles to failure (N). The curves are often plotted on a log-log plot, which displays an approximate linear relationship between the stress amplitudes and the number of cycles to failure. This linear relationship can be written as,

$$N = B/S_m \quad (1)$$

Where S_m = nominal stress range at a fatigue sensitive detail; N = number of stress cycles to fatigue failure; B = detail category constant, varying with type of detail. Thus, the S-N curve is used to estimate the number of cycles a material can withstand until failure, also known as the fatigue life.

The S-N curve provides meaningful results when used in collaboration with the stress range histograms from testing, as illustrated in Figure 71. The stress range histogram presents the occurrence of stress cycles in terms of the number of cycles for each stress range magnitude captured during the measurement period.

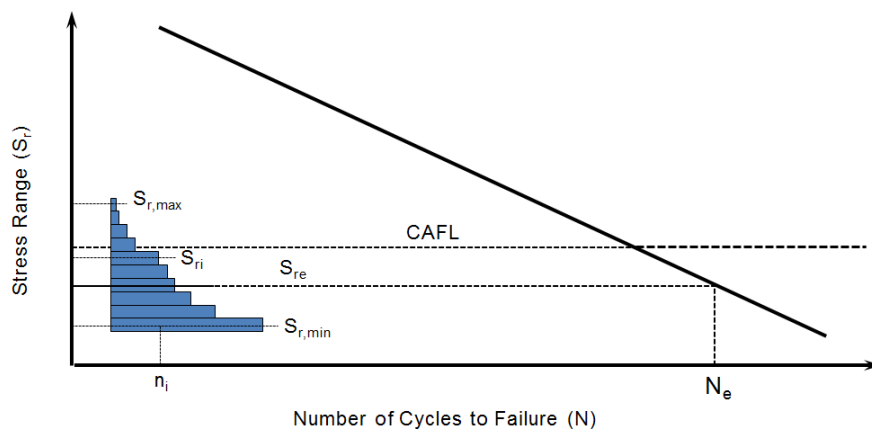


Figure 71 - Stress Range Histogram Used with an S-N curve

The compilation of these various stress ranges are used to calculate the number of loading cycles a bridge component can experience until failure is reached. When considering constant amplitude loads, the stress range calculation is simply the minimum stress value subtracted from the maximum stress value. However, the traffic loading on a bridge is sporadic in nature and is classified as a variable amplitude loading type. Since fatigue strength S-N curves were previously developed under constant-amplitude cyclic loading, the general approach in

assessing the effects from traffic loads is to determine an effective stress range from the corresponding stress cycles. For steel structures, the root-mean cube stress range, Equation 2, calculated from a variable amplitude stress range histogram has been found to produce the best results (Zhou, 2006).

$$S_{re} = (\sum D_i S_i^3)^{1/3} \quad (2)$$

Where S_{re} is the effective stress range of a variable amplitude stress range histogram, S_i is the i th stress range in the stress range histogram; $D_i = n_i / N_{Total}$, fraction of occurrence of stress range S_i in the histogram, $n_i =$ number of occurrences of stress range S_i , and $N_{Total} =$ total number of occurrences of all stress cycles in the histogram.

The rainflow cycle counting method has been used to display the time-varying stress history against the number of cycles (n_i). The fatigue life ($n_{f,i}$) corresponding to the number of cycles to failure at the specific stress event is estimated from the S-N diagram. The fatigue damage (D_i) for each cycle and half-cycle is written as (n_i / N), as displayed in Equation 3. The Palmgren-Miner linear damage rule is then used to calculate the accumulated damage, which assumes fatigue damage occurs when the sum of the cycle ratios at each constant amplitude stress event reaches a critical damage value (DPM).

$$D_i = \frac{n_i}{N} \text{ for } i = 1, \dots, k \quad (3)$$

The cumulative damage function is estimated using full range Miner rule with the omission of the cycles with amplitude lower than the endurance limit.

$$C_i = \sum_{n=1}^i D_n \text{ for } i = 1, \dots, k \quad (4)$$

Where C_i is the cumulative damage function, assuming that the damage accumulates in the material in a linear way

5.3.2 Fatigue Predictions, Crack Growth Modeling

Once a fatigue crack has initiated, applied repeated stresses cause propagation of a crack across the section of the member until the crack grows to a size where the member is capable of fracture. While the nature of a material cracking is a non-elastic deformation, the region beyond the crack (at the crack tip) experiences a linear elastic stress field under load. This local crack tip stress field is related to the remotely applied stress on the structural element. Paris model is most widely used model for the prediction of crack growth. In this model, the range of the stress intensity factor (ΔK) is the main factor driving the crack growth with two parameters C and m that reflect the material properties.

$$\frac{da}{dN} = C(\Delta K)^m \quad (5)$$

Where a is the initial crack size, N is the number of fatigue loading cycles, C and m are material properties, and ΔK is the stress intensification factor.

Certain features of acoustic emission signals are stochastically correlated with crack growth model variables, such as stress intensity factor, ΔK , and crack growth rate da/dN . Two of the more commonly used AE parameters that are associated with crack growth are the AE count, c , and its derivative, count rate, dc/dN . The following formulation is proposed for the relationship between the AE event or AE count rate, dc/dN and the stress intensity factor, ΔK :

$$\frac{dc}{dN} = A_1(\Delta K)^{A_2} \quad (6)$$

Where c is defined as the number of times that a signal amplitude exceeds a predefined threshold value, and A_1 and A_2 are the model parameters and mainly depend on material properties. This equation can be rearranged to solve for ΔK and taking the log of both sides will yield a linear relationship between ΔK and dc/dN :

$$\log \Delta K = \alpha_1 \log \left(\frac{dc}{dN} \right) + \alpha_2 \quad (7)$$

Where $\alpha_1 = A_1^{-1/A_2}$ and $\alpha_2 = 1/A_2$ are the new model constants to be determined experimentally from data. Thus, only the AE count data is needed to estimate and solve for the stress intensity factor, the driving force in crack growth modeling.

The stress intensity factor displays the same log-linear behavior with the AE count rate, dc/dN , as it does with the crack growth, da/dN . Therefore, substituting into the Paris equation gives the following relationship:

$$\log \frac{da}{dN} = \beta_1 \log \left(\frac{dc}{dN} \right) + \beta_2 \quad (8)$$

Where β_1 and β_2 are the model parameters that describe the log-linear relationship between AE count rate and crack growth.

The estimation of ΔK through the use of acoustic emission signals removes the need for complex modeling that is typically used in fracture mechanics to calculate stress intensity factors. These computations become especially difficult for 3-dimensional cases with curved crack fronts, such as the curvature in a welded connection. While calculations are possible, extensive computer capacity and experience is often required. Nonetheless, the relationship between the AE events and crack growth rate means that the rate of crack growth can be estimated solely on features of the AE signals.

5.3.3 Probabilistic Modeling

Bayesian updating allows the use of dynamic diagnostic information with prior knowledge for improved prognosis. The Bayesian nets will be developed to update and inter-correlate the probabilistic deterioration model parameters associated with the limit states for the selected

bridge structural components. For fatigue limit state, the Paris law with two probabilistic parameters (i.e., initial crack length, a_0 , and random variable, C) is used in steel bridges with fatigue failures. By incorporating the probabilistic structural deterioration model with Bayesian nets, more accurate updated RUL can be predicted and optimal maintenance strategies are made accordingly.

The variables that account for material properties in the crack growth model are critical factors to determine the growth of damage. The uncertainties in these variables may be large due to manufacturing and aging of the material. This is especially true on welded connections that may contain defects or internal discontinuities such as porosity (trapped gases in the unfused area expanding and getting trapped in the solidifying weld), or incomplete fusion.

Since Paris law is based on crack growth during N cycles, the crack growth data is used to initially characterize the material properties, C and m . The probability distribution of these variables is used to account for the uncertainties. The following form of Baye's theorem can be used to solve for these distributions:

$$f_{\text{updt}}(m) = \frac{P(\Delta a|m)f_{\text{ini}}(m)}{\int_{-\infty}^{+\infty} P(\Delta a|m)f_{\text{ini}}(m)dm} \quad (9)$$

Where, if m is the variable we want to update, f_{ini} , the assumed (or prior) probability density function (PDF) of m , and $P(\Delta a|m)$ is called the likelihood function, which is the probability of obtaining the measured damage growth, Δa , for a given value of m . The updating of these variables allows distributions to be narrowed and converged to true values. Through the determination of the probability distribution of these variables, the RUL can be estimated.

Ultimately, the computation of RUL through fatigue prediction models, crack growth modeling, and probabilistic models, can be integrated together to determine the amount of damage. The

conclusions from these analyses offer bridge owners with more meaningful conclusions and information. Knowing the right time to repair or replace infrastructure has the added benefit of making the most cost-effective decisions.

5.3.4 SHM integrated with BIM

A framework of SHM integrated with BIM (bridge information modeling) was developed using Revit Structures software to illustrate sensor data storage and display, finite element simulation, and structural condition assessment integrated in a BIM-enabled 4D setting, as shown in Figure 72. The framework includes the following four major modules: BIM model and a database, SHM portal, sensor clusters that automates the activation of the relevant area in the BIM model, and finite element simulation software. The SHM framework integrated with BIM can significantly reduce the amount of time that would be spent performing searching, accessing and validating the information. A 3D BIM model for the monitored structure provides a visual clue about the location and condition of the key monitoring area and associated sensor clusters. This facilitates the visualization of the processed SHM information and its variation with time. In this way, a 4D model that integrates a 3D drawing with time is made available and allows the consideration of maintenance actions for deteriorating structural components through their life cycle. Changes that occur in the structural condition and SHM system over time can be highlighted in such a 4D BIM model. Furthermore, structural safety can be quantified in terms of structural reliability, taking into account the uncertainty involved. A prototype ISHM system including the BIM model, a FE analysis software, sensors and custom-developed middleware code (i.e. BIM for SHM portal), are shown in Figure 72. The I-270 Middlebrook Bridge was built in 1980's and fatigue cracks were identified in some of the

diaphragm connection welds. Types of sensors used in the field test include piezoelectric film AE sensors, wireless accelerometers, laser distance sensors and strain transducers.

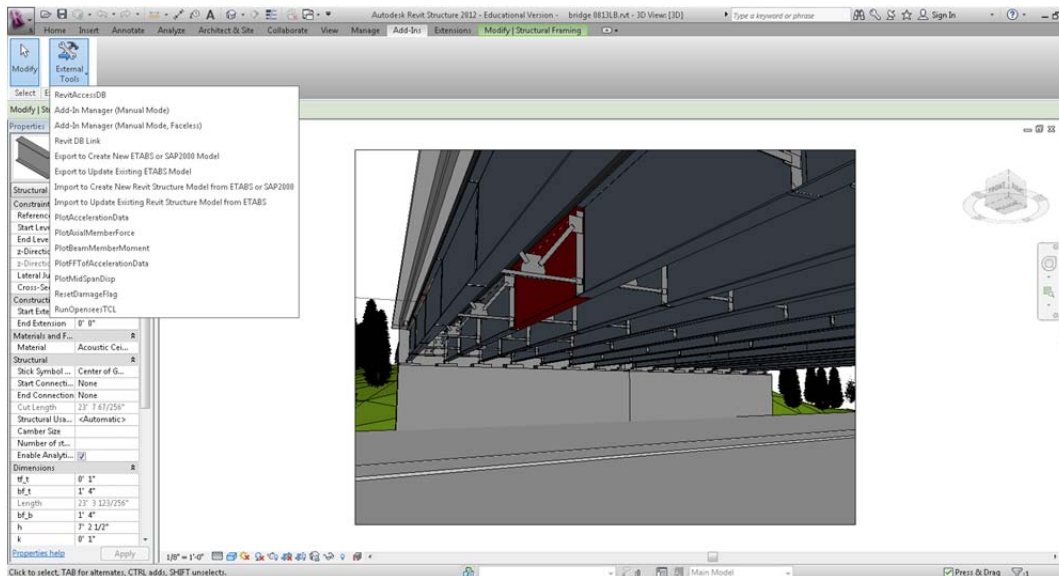


Figure 72 - BIM model of the prototype steel highway bridge

Since the ultimate goal of SHM is to evaluate the structural safety of the monitored structure, a 4D BIM model with time varying structural condition and system reliability information is highly desired for decision making in the SHM applications. A time-dependent reliability analysis requires the knowledge of deterioration models which predict the future structural condition and form the basis for life-cycle monitoring and maintenance planning. The models must be updated over time to revise the optimum maintenance strategy based on how a structure actually behaves. Sensor data from the SHM system installed on the monitored structure has been shown to be very useful for updating the deterioration models for future condition forecasting. Condition rating data based on periodic inspection of bridges components provides an overall characterization of the general condition of a bridge that has been routinely used by inspection engineers. The condition data for each element is recorded and stored in a database,

which could be displayed in the BIM environment at user's request for selected element as shown in Figure 72. To illustrate the concept, condition rating along with a Markovian-based modeling approach for estimating the deterioration of condition states of structural elements is adopted in this study. Markovian-based model is one of the most popular methods for bridge deterioration modeling and have been used by major Bridge Management System software including PONTIS. A Markov chain is a stochastic process in which the probability distribution in the next time point depends only on the current state. The Markovian transition matrix reflects the typical deterioration rates of the bridges in the dataset. Once updated with monitoring data, they can be used to forecast the future condition states of the monitored structural components. With visual display of the structural condition in the BIM model, the bridge owner can make more intelligent and cost-effective decisions related to preserving their bridge assets with timely maintenance actions.

6.0 Task 6: Project Website, Report and Project Assessment

A project website hosted at the UMD was established at the onset of the project and kept updated throughout. The link address is <http://ishm.umd.edu/>. Quarterly reports were submitted since the first quarter (July 15th to October 14th, 2011.) This final progress report summarizes the results of the technical assessment and evaluation and is submitted as deliverable of this task. Also this report discusses the results of the economic evaluation of the project. The MdDOT and NCDOT provided in-kind supports of \$305,000 and \$240,000, respectively, to implement the technology and make the system ready for commercialization. Strategy of commercialization has been consulted to the TAC, BEST Center industrial partners, Offices of Technology Commercialization (OTC) of UMD and NCSU, and other DOTs.

On June 23, 2014, the UMD research team (Drs. Fu and Zhang) met with the staff members from the Office of Technology Commercialization (OTC) of the University of Maryland. The two OTC staff members are Pasquale Ferrari, a Licensing Associate and Marck-Arthur Clerveau, Physical Sciences Licensing Analyst. During the meeting, Dr. Fu presented the project research work/outcomes and potential sensor and crack detection technologies for licensing. Mr. Ferrari explained the OTC procedure for technology licensing and encouraged the project team to discuss with potential technology transfer partners for licensing.

Guests from the Maryland Department of Transportation were invited to the demo site at I-95 over Patuxent River, Laurel, MD. The whole process was performed to showcase the wireless smart sensor system with piezo paint AE sensors and hybrid-mode energy harvester. Also demonstrated were the pencil break tests to simulate the fatigue cracks to different groups of guests from Maryland State Highway Administration (MDSHA) and Maryland Transportation

Authority (MDTA). The open day on May 22nd, 2014 was to demonstrate the AE sensor and crack detection technology and explain the benefits of the system to the bridge owners.

Below listed in Table 2 is the summarization of the final status of the twelve deliverables listed in the proposal Attachment 2 as well as Chapter 1 of this report.

Table 2 - Summary of the Final Status of Twelve Deliverables	
Deliverable	Item
1	<ul style="list-style-type: none"> The technical advisory committee (TAC) was formed and kick-off team meeting was conducted on August 5, 2011. Baseline field test procedure on Paint Branch Bridge on US Route 1 was conducted in the first quarter to experimentally determine the environmental and bridge parameter values for ISHM system. Remote sensing requirements and prognostics procedure for the proposed ISHM system were developed in the first quarter.
2	<ul style="list-style-type: none"> Project website hosted at the University (ishm.umd.edu) was established in the first quarter and periodically updated throughout the project period (2011-2014)
3	<ul style="list-style-type: none"> Findings of the all activities performed under Task 1 (finite element model, sensor placement scheme, environmental variable data, etc.) and details of baseline test on the Paint Branch Bridge on US Route 1 were reported and made available on the project website in the second quarter.
4	<ul style="list-style-type: none"> Findings of the all activities performed under Task 2 (piezo paint sensor with improved sensitivity, reconfigurable piezo paint sensor dots), description of corresponding development procedure for modeling, fabrication, and experimental characterization of piezo paint AE sensor were reported and made available on the project website from the second to the fourth quarters.
5	<ul style="list-style-type: none"> The status of research efforts and findings in virtual T-R experiments and lab tests to validate and characterize T-R method for fatigue related damage detection were reported periodically throughout the project.
6	<ul style="list-style-type: none"> Self-sustained wireless smart sensor and hybrid-mode energy harvester were developed in the extended third year. Findings of the all activities performed under this task were reported and made available on the project website from the eighth to the twelfth quarters
7	<ul style="list-style-type: none"> The status of research efforts and findings in wireless smart sensor and onboard diagnostics method based on the T-R algorithm were reported. The wireless smart sensor system were validated and evaluated through corresponding lab tests. Both works were extended to the third year, reported and made available on the project website from the eighth to the twelfth quarters.

8	<ul style="list-style-type: none"> • Integrated piezo paint AE sensors with wireless smart sensor and hybrid-mode energy harvester were validated and thoroughly evaluated through lab tests and field tests on real bridges • The work was extended to the third year, reported and made available on the project website from the ninth to the twelfth quarters.
9	<ul style="list-style-type: none"> • The research efforts and findings in lab tests and field tests of the ISHM system were extended to the third year, reported and made available on the project website from the ninth to the twelfth quarters.
10	<ul style="list-style-type: none"> • Strategy to incorporate remote sensing and prognosis of bridge components into bridge management system was reported and made available on the project website in the sixth quarter. It has been thought through the whole project.
11	<ul style="list-style-type: none"> • Quarterly status and progress reports were submitted every quarters of 2011- 2014 and final project report is enclosed.
12	<ul style="list-style-type: none"> • Paper submissions to conference presentations and publication to TRB meeting or other pipeline conferences with recognition of this project are listed here <ol style="list-style-type: none"> 1. Zhou, C. and Zhang, Y. (2012), "Steel Bridge Fatigue Crack Monitoring with Broadband Thin-film AE Sensors," <i>Proc. 6th International Conference on Bridge Maintenance, Safety and Management (IABMAS 2012)</i>, Stresa, Lake Maggiore, Italy, July 8-12, 2012. 2. Fu, C.C., Zhang, Y., Yuan, F.G., Zhou, E. (2012), "Integration of Self-sustained Wireless Structural Health-Monitoring System for Highway Bridges," The Transportation Research Board, 91st Annual Meeting, Jan. 22, 2012, Washington, DC 3. Drs. C. C. Fu & Y. Zhang of UMD and F.G. Yuan of NCSU interviewed by ASCE Civil Engineer Magazine and article appeared in April 2012 issue under Technology section titled "Structural Health Monitoring Tests Planned for Bridges." 4. Chen, C.L., Liu, Y.L., and Yuan, F.G. (2012), "Impact Source Identification of Isotropic Plate Structures using Time-Reversal Method: Experimental Study," <i>Smart Materials and Structures</i>, Vol. 21, 105025, 2012. 5. Zhang, Y. F., Zhou, C., Fu, C.C. and Zhou, E. (2013), "Field Monitoring of Fatigue Crack on Highway Steel I-Girder Bridge," (13-4097) the <i>Proceedings of Transportation Research Board</i>, January 13-17, 2013, Washington, D.C. 6. Zhou, C. (2013). Fatigue crack monitoring with coupled piezoelectric film acoustic emission sensors, Doctoral Dissertation, Department of Civil and Environmental Engineering, University of Maryland, College Park, Maryland 7. Fu, C.C.; Zhao, G.; Saad, T.; Zhang, Y.; Zhou, Y.E. (2014); "Fatigue Crack Detection and Evaluation in a Welded Steel Girder Highway Bridge," <i>the</i>

	<p><i>proceedings of 7th International Conference on Bridge Maintenance, Safety and Management (IABMAS2014)</i>, July 7-11, 2014, Shanghai, China</p> <p>8. Fu, C.C.; Zhao, G.; Saad, T.; Zhang, Y.; Zhou, Y.E. (2014); "Investigation of Fatigue-induced Crack with K-type Bracing System," <i>the proceedings of iBridge Conference 2014</i>, August 11-13, 2014, Istanbul, Turkey</p> <p>9. Zhou, C. and Zhang, Y. (2014). "A coupled acoustic emission (AE) sensor system for near-field AE source localization," <i>J. of Intelligent Material System and Structures</i>, published online on January 3, 2014, pp. 1-11</p> <p>10. Zhou, C. and Zhang, Y. (2014). "Near-field acoustic emission sensing performance of piezoelectric film strain sensor," <i>Research in Nondestructive Evaluation</i>, 25(1): 1-19.</p> <p>11. Zhu, J. T.; X. C. Zhang; C. Wan; L. Liu; L. Shu; Z. D. Xu; W. S. Zhou; F. G. Yuan (2015), "Development a self-contained wireless based SHM system for monitoring a Swing bridge," <i>International Journal of Sustainable Materials and Structural Systems</i>, 2015 (accepted)</p>
--	--

7.0 Findings/Conclusions

Based on the previous discussed six tasks, a functioning wireless Integrated Structural Health Monitoring (ISHM) System with remote sensing, diagnostics and prognosis was developed, tested in the lab as well as in the field, deployed and validated. This chapter is to summarize all the works and achievements.

Findings by tasks are listed here:

1. Findings of all activities of deliverables 3 performed under Task 1 (finite element model, sensor placement scheme, environmental variable data, etc.) were all accomplished timely.
2. Findings of all activities of deliverable 4 performed under Task 2 (piezo paint sensor with improved sensitivity, reconfigurable piezo paint sensor dots) were all accomplished timely.
3. Findings of the all activities of deliverables 5, 6, and 7 performed under Tasks 3 and 4 (onboard diagnostics method based on the T-R algorithm, self-sustained wireless smart sensor and hybrid-mode energy harvester) were completed in the extended third year due to:
 - a. Although T-R method was well tested and validated in the lab by the research team, due to the more complicated configuration of bridge components and field noise, it needed further post-process to sort out the orientation and location of the crack source.
 - b. Field Programmable Gate Arrays (FPGAs) is the key part of the wireless sensor board. When the contract was awarded, a proto-type of the wireless system was ready then. Unfortunately, due to the volatility of the market, the early-adopted FPGA part was no longer available for batch production of the wireless sensor board and a new FPGA part has to be used which has been successfully integrated into the wireless

sensor board. But this modified design took the research team some time to fabricate, programming and test.

4. Findings of all activities in lab tests and field tests of the ISHM system of deliverables 8 and 9 performed under Task 5 (integrated piezo paint AE sensors with wireless smart sensor and hybrid-mode energy harvester) were completed in the extended third year due to
 - a. Selecting four testing (baseline, demo and pilot) bridges in the States of Maryland and North Carolina and accommodation to the State Highway Agency's' inspection cycle;
 - b. Loss of sensor, communication and power due to environmental impact (moisture, noise, grounding, etc.) during field test. Improvement on the sensor packaging and weather-proof was made.
 - c. Unexpected incidences, such as vandalism and accidentally unplugged chord by maintenance workers;
 - d. Modified design of the wireless sensor board due to discontinued part (as described in item 3 above.)
5. Finding of strategy to incorporate remote sensing and prognosis of bridge components into bridge management system of deliverable 10 performed under Task 5.3 were considered and reported.
6. Administrative requirements of all activities of deliverables 1 (technical advisory committee), 2 (website), 11 (quarterly and final progress reports) and 12 (presentation and paper submission) under Tasks 1 and 6 were all performed timely.

In summary, a functioning wireless Integrated Structural Health Monitoring (ISHM) System with remote sensing, diagnostics and prognosis was developed, tested in the lab as well as in the

field, deployed and validated. Major tasks have been fulfilled. Deliverables have been timely submitted or exercised within the extended period of 36 months. Work associated with commercialization was conducted with limited success, but all visitors/guests concur the ISHM system has an enormous potential for the bridge health monitoring and its advancement.

Although the research team has accomplished a lot through this project, there are still some future actions and recommendations to make here:

1. Future improvements of the sensor preamplifier/filter circuitry could be made to further reduce the noise floor to below 2 mV.
2. Current study is limited to using piezoelectric AE film sensor for fatigue crack monitoring in steel structures. Experimental study of the sensing performance of piezoelectric film AE sensor on different structural materials, such as reinforced concrete and fiber reinforced polymer composite bridge deck structures, would be of interest for future consideration.
3. Even though AE sensors have been proved as a useful tool for fatigue crack detection, there is a need to establish a quantitative relationship between J-integral near the crack tip zone and acoustic emission signals collected by piezo film AE sensors.
4. Although T-R method was well tested and validated in the lab by the research team, there is a need to make it efficient for the onboard interrogation and identification for fatigue crack signals at bridge sites.
5. Although all visitors to the demo bridge sites were impressed with the system and how it functioned, work associated with commercialization was conducted with limited success. More educational and promotional works are needed, maybe in the national level.

Attachment 1

Wireless ISHM

Wireless ISHM

Wireless ISHM

Technical and Deliverable Milestone Schedule								
Item No.	Task No.	Activity/Deliverable	Quarter No.	Expected Completion Date/Mos	Payable Milestone	Projected Federal Payment	Projected Partner Cost-Sharing	Total
(per proposal)		<u>ACTIVITY/DELIVERABLE</u>	<u>TITLE</u>					
1	1	#1 & #3. Perform baseline field test on bridges to obtain data for sensor & energy harvester development & implementation	1	3 months	Completion of determining values of parameters (i.e., noise level, energy intensity, measurement range, wind, moisture, traffic) to support sensor, energy harvester and ISHM system (software & hardware) design	\$20,000	\$50,000	\$70,000
2	2	#4. Design piezo paint acoustic emission (AE) sensor with reconfigurable sensing dots	1	12 months	Completion of design drawing and fabrication method for making peelable layer with reconfigurable sensing dots	\$25,000	\$30,000	\$55,000
3	3	#5. Develop and evaluate time-reversal (T-R) method for AE source identification	1	12 months	Completion of TR algorithm for AE source identification development and numerically verification(virtual T-R experiments completed)	\$25,000	\$26,755	\$51,755
4	6	#2. Establish a project website	1	24 months	Establishment of a project website hosted at the University	\$10,000	\$0	\$10,000
5	6	#11. 1st Quarterly Status Report	1	3 months	Submit 1st quarterly report	\$582	\$0	\$582
First Payable Milestone			1	3 months	SUBTOTAL (7% project completed)	\$80,582	\$106,755	\$187,337
6	2	#4. Fabricate piezo paint acoustic emission (AE) sensor with reconfigurable sensing dots	2	12 months	Completion of large area (3" wide roll) piezo paint AE sensor with reconfigurable sensing dots fabricated	\$20,000	\$30,000	\$50,000
7	3	#5. Evaluate time-reversal (T-R) method for AE source identification by conducting lab experiments	2	12 months	Verification of TR algorithm for AE source identification on steel plate specimens in lab	\$20,000	\$30,000	\$50,000
8	4	#6. Develop wireless smart sensor and hybrid-mode energy harvester	2	12 months	Completion of design for wireless sensor and hybrid-mode energy harvester	\$20,000	\$22,005	\$42,005
9	5	#10. Develop ISHM system for bridge management	2	36 months	Completion of prototype system design for ISHM	\$30,000	\$40,000	\$70,000
10	6	#11. 2nd Quarterly Status Report	2	6 months	Submit 2nd quarterly report Completion of Task 1)	\$2,093	\$0	\$2,093
Second Payable Milestone			2	6 months	SUBTOTAL (15% project completed)	\$92,093	\$122,005	\$214,098
11	2	#4. Evaluate piezo paint acoustic emission (AE) sensor with reconfigurable sensing dots	3	12 months	Completion of characterization results for evaluating piezo paint sensitivity, bandwidth, and eletromechanical properties (d31 factor, modulus, impedance)	\$15,000	\$20,000	\$35,000
12	3	#5, Evaluate time-reversal (TR) method for AE source identification by conducting lab experiments	3	18 months	Completion of TR algorithm for AE source identification verified on steel plate specimens with fatigue cracks	\$15,000	\$20,000	\$35,000

Attachment 1

Wireless ISHM

Wireless ISHM

Wireless ISHM

Technical and Deliverable Milestone Schedule								
Item No.	Task No.	Activity/Deliverable	Quarter No.	Expected Completion Date/Mos	Payable Milestone	Projected Federal Payment	Projected Partner Cost-Sharing	Total
(per proposal)		<u>ACTIVITY/DELIVERABLE</u>			<u>TITLE</u>			
13	4	#6. Develop wireless smart sensor and hybrid-mode energy harvester	3	12 months	Completion of wireless smart sensor and hybrid-mode energy harvester fabricated	\$20,000	\$36,000	\$56,000
14	5	#10. Develop ISHM system for bridge management	3	36 months	Development of fatigue life prognosis method for incorporation into ISHM system developed for bridge management	\$30,000	\$30,755	\$60,755
15	6	#11. 3rd Quarterly Status Report	3	9 months	Submit 3rd quarterly report	\$582	\$0	\$582
		Third Payable Milestone	3	9 months	SUBTOTAL (22% project completed)	\$80,582	\$106,755	\$187,337
16	2	#4. Characterize piezo paint acoustic emission (AE) sensor with reconfigurable sensing dots	4	12 months	Completion of characterization results for evaluating piezo paint AE sensor with reconfigurable sensing dots on lab specimens (steel plates with fatigue cracks)	\$30,000	\$40,000	\$70,000
17	3	#5. Evaluate time-reversal (TR) method for AE source identification by conducting fatigue tests in lab	4	12 months	Completion of verification results for TR method with piezo paint AE sensors on steel plate specimens under fatigue loading	\$20,000	\$30,000	\$50,000
18	4	#6. Develop and experimentally evaluate wireless smart sensor and hybrid-mode energy harvester	4	12 months	Completion of characterization results for wireless tape sensor and hybrid-mode energy harvester in lab tests	\$20,000	\$32,005	\$52,005
19	5	#10. Develop ISHM system for bridge management	4	36 months	Completion of prototype ISHM system for bridge management developed and verified in lab environment	\$20,000	\$20,000	\$40,000
20	6	#11. 4th Quarterly Status Report	4	12 months	Submit 4th quarterly report (Completion of Tasks 2 & 3)	\$2,093	\$0	\$2,093
		Fourth Payable Milestone	4	12 months	SUBTOTAL (30% project completed)	\$92,093	\$122,005	\$214,098
21	2	#6 & #9. Field test of piezo paint acoustic emission (AE) sensor with reconfigurable sensing dots	5	18 months	Completion of field test data in implementing piezo paint AE sensor on steel I-girder bridge	\$20,000	\$30,000	\$50,000
22	4	#7 & #9. Field test of time-reversal (TR) method for AE source identification by conducting fatigue	5	24 months	Verification of TR method with piezo paint AE sensor on steel I-girder bridge	\$20,000	\$30,000	\$50,000
23	4	#8. Integrate wireless smart sensors and hybrid-mode energy harvester with piezo paint AE sensor	5	30 months	Data collection from piezo paint AE sensor integrated with wireless tape sensor and hybrid-mode energy harvester on steel I-girder bridge	\$20,000	\$30,000	\$50,000

Attachment 1

Wireless ISHM

Wireless ISHM

Wireless ISHM

Technical and Deliverable Milestone Schedule								
Item No.	Task No.	Activity/Deliverable	Quarter No.	Expected Completion Date/Mos	Payable Milestone	Projected Federal Payment	Projected Partner Cost-Sharing	Total
(per proposal)		<u>ACTIVITY/DELIVERABLE</u>			<u>TITLE</u>			
24	5	#10. Develop ISHM for bridge management	5	36 months	Completion of prototype ISHM system for bridge management developed for field implementation	\$20,000	\$16,755	\$36,755
25	6	#11. 5th Quarterly Status Report	5	15 months	Submit 5th quarterly report	\$582	\$0	\$582
Fifth Payable Milestone			5	15 months	SUBTOTAL (37% project completed)	\$80,582	\$106,755	\$187,337
26	2	#6 & #9. Field test of piezo paint acoustic emission (AE) sensor with reconfigurable sensing dots	6	18 months	Completion of field test data in implementing piezo paint AE sensor on steel truss bridge	\$30,000	\$40,000	\$70,000
27	4	#7 & #9. Field test of time-reversal (TR) method for AE source identification by conducting fatigue tests	6	24 months	Verification of TR method with piezo paint AE sensor on steel truss bridge	\$20,000	\$20,000	\$40,000
28	4	#8. Integrate wireless smart sensors and hybrid-mode energy harvester with piezo paint AE sensor	6	30 months	Data collection from piezo paint AE sensor integrated with wireless tape sensor and hybrid-mode energy harvester on steel truss bridge	\$20,000	\$32,005	\$52,005
29	5	#10. Field implementation of ISHM system for bridge management	6	36 months	Completion of remote monitoring functionality of prototype ISHM system for bridge management developed for field test	\$20,000	\$30,000	\$50,000
30	6	#11. 6th Quarterly Status Report	6	18 months	Submit 6th quarterly report (Completion of Task 4)	\$2,093	\$0	\$2,093
Sixth Payable Milestone			6	18 months	SUBTOTAL (45% project completed)	\$92,093	\$122,005	\$214,098
31	4	#9 & #8. Field test of piezo paint AE sensors integrated with wireless tape sensors and hybrid-mode energy harvester	7	36 months	Evaluation of the accuracy of piezo paint AE sensor integrated with wireless tape sensor and hybrid-mode energy harvester in AE source location on real bridges	\$40,000	\$50,000	\$90,000
32	5	#10. Field test of ISHM system for bridge management	7	36 months	Evaluation of ISHM system performance for bridge management with field test data in item 31	\$40,000	\$56,754	\$96,754
33	6	#11. 7th Quarterly Status Report	7	21 months	Submit 7th quarterly report (Completion of Task 5)	\$582	\$0	\$582
Seventh Payable Milestone			7	21 months	SUBTOTAL (52% project completed)	\$80,582	\$106,754	\$187,336
34	4	#9 & #8. Field test of piezo paint AE sensors integrated with wireless tape sensors and hybrid-mode energy harvester	8	36 months	Evaluation of the accuracy of piezo paint AE sensor integrated with wireless tape sensor and hybrid-mode energy harvester in AE source location on real bridges	\$40,000	\$60,000	\$100,000
35	5	#10. Field test of ISHM system for bridge management	8	36 months	Evaluation of ISHM system performance for bridge management with field test data in item 31	\$50,000	\$62,005	\$112,005
36	6	#11. 8th Quarterly Status Report	8	24 months	Submit 8th quarterly report (Completion of Task 5)	\$2,094	\$0	\$2,094
Eighth Payable Milestone			8	24 months	SUBTOTAL (60% project completed)	\$92,094	\$122,005	\$214,099

Attachment 1

Wireless ISHM

Wireless ISHM

Wireless ISHM

Technical and Deliverable Milestone Schedule								
Item No.	Task No.	Activity/Deliverable	Quarter No.	Expected Completion Date/Mos	Payable Milestone	Projected Federal Payment	Projected Partner Cost-Sharing	Total
(per proposal)		<u>ACTIVITY/DELIVERABLE</u>						
		<u>TITLE</u>						
37	4	#9 & #8. Field test of piezo paint AE sensors integrated with wireless tape sensors and hybrid-mode energy harvester	9	36 months	Evaluation of the accuracy of piezo paint AE sensor integrated with wireless tape sensor and hybrid-mode energy harvester in AE source location on real bridges	\$50,000	\$70,000	\$120,000
38	5	#10. Field test of ISHM system for bridge management	9	36 months	Evaluation of ISHM system performance for bridge management with field test data in item 31	\$64,000	\$82,506	\$146,506
39	6	#11. 9th Quarterly Status Report	9	27 months	Submit 9th quarterly report (Completion of Task 5)	\$1,117	\$0	\$1,117
Ninth Payable Milestone			9	27 months	SUBTOTAL (70% project completed)	\$115,117	\$152,506	\$267,623
40	4	#9 & #8. Field test of piezo paint AE sensors integrated with wireless tape sensors and hybrid-mode energy harvester	10	36 months	Evaluation of the accuracy of piezo paint AE sensor integrated with wireless tape sensor and hybrid-mode energy harvester in AE source location on real bridges	\$50,000	\$70,000	\$120,000
41	5	#10. Field test of ISHM system for bridge management	10	36 months	Evaluation of ISHM system performance for bridge management with field test data in item 31	\$64,000	\$82,506	\$146,506
42	6	#11. 10th Quarterly Status Report	10	30 months	Submit 10th quarterly report (Completion of Task 5)	\$1,117	\$0	\$1,117
Tenth Payable Milestone			10	30 months	SUBTOTAL (80% project completed)	\$115,117	\$152,506	\$267,623
43	4	#9 & #8. Field test of piezo paint AE sensors integrated with wireless tape sensors and hybrid-mode energy harvester	11	36 months	Evaluation of the accuracy of piezo paint AE sensor integrated with wireless tape sensor and hybrid-mode energy harvester in AE source location on real bridges	\$50,000	\$70,000	\$120,000
44	5	#10. Field test of ISHM system for bridge management	11	36 months	Evaluation of ISHM system performance for bridge management with field test data in item 31	\$64,000	\$82,506	\$146,506
45	6	#11. 11th Quarterly Status Report	11	33 months	Submit 11th quarterly report (Completion of Task 5)	\$1,117	\$0	\$1,117
Eleventh Payable Milestone			11	33 months	SUBTOTAL (90% project completed)	\$115,117	\$152,506	\$267,623
46	4	#9 & #8. Field test of piezo paint AE sensors integrated with wireless tape sensors and hybrid-mode energy harvester	12	36 months	Evaluation of the accuracy of piezo paint AE sensor integrated with wireless tape sensor and hybrid-mode energy harvester in AE source location on real bridges	\$41,117	\$70,000	\$111,117
47	5	#10. Field test of ISHM system for bridge management	12	36 months	Evaluation of ISHM system performance for bridge management with field test data in item 31	\$56,000	\$82,506	\$138,506

Attachment 1

Wireless ISHM

Wireless ISHM

Wireless ISHM

Technical and Deliverable Milestone Schedule								
Item No.	Task No.	Activity/Deliverable	Quarter No.	Expected Completion Date/Mos	Payable Milestone	Projected Federal Payment	Projected Partner Cost-Sharing	Total
(per proposal)		<u>ACTIVITY/DELIVERABLE</u>			<u>TITLE</u>			
48	6	#10. Draft a set of recommendations to be submitted to the relevant organizations for future adoption into bridge management practice	12	36 months	Submittal of a set of clear, concise recommendations to the appropriate organizations (e.g., MDOT, FHWA, NCDOT) for incorporation into the relevant consensus guides and recommended practices manuals for bridge management	\$15,000		\$15,000
49	6	#11. Prepare and Submit Draft Final Report	12	36 months	Submit draft final report	\$3,000	\$0	\$3,000
		Twelveth Payable Milestone	12	36 months	SUBTOTAL (100% project completed)	\$115,117	\$152,506	\$267,623
50	6	#11. Address Comments and Submit Final Report	13	36 months	Submit final report	\$0	\$0	\$0
51	6	#12. Prepare & Present Paper at public event	n/a	36 months	Preparation & Presentation of Paper at public event	\$0	\$0	\$0
52	6	#11. Peer Review - Washington, DC January or February Annually	n/a	36 months	Preparation of presentation & Submittal of presentation file.	\$0	\$0	\$0
SUBTOTAL						\$0	\$0	\$0
GRAND TOTALS						\$1,151,169	\$1,525,063	\$2,676,232